Chapter 2

Investigation of N,N'-Disulfopiperazinium Chlorometallates as Hybrid Catalysts for the Synthesis of 1,2-Dihydroquinazoline Derivatives

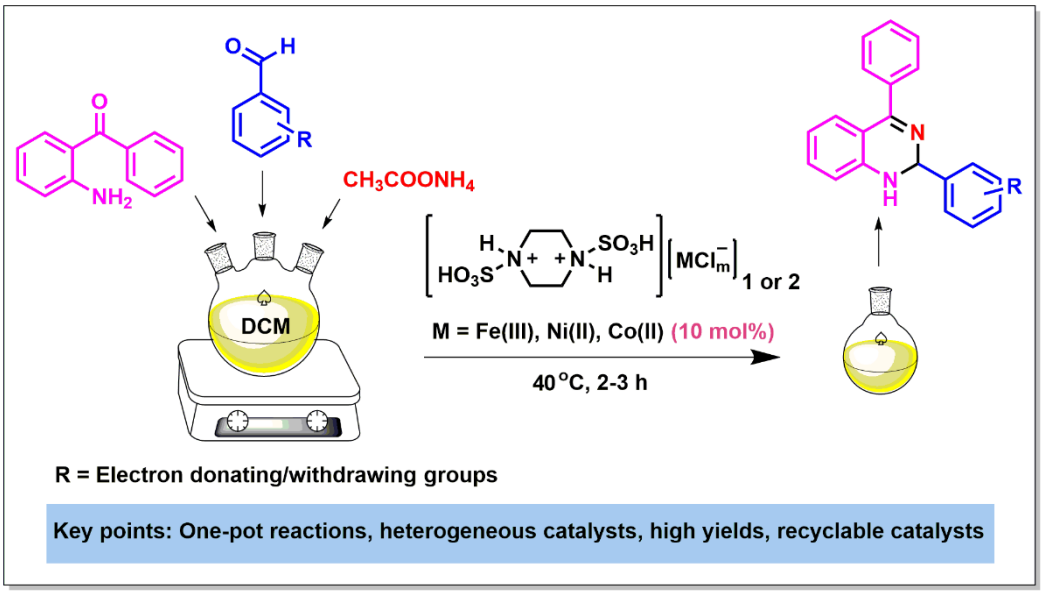

Synopsis

Three Brønsted-Lewis acidic halometallates of N,N'-disulfopiperazinium cation with complex metal chloride anions of Fe(III), Ni(II) and Co(II) were developed as solid materials. Various spectrochemical techniques like FT-IR, UV-Visible, SEM, EDX, Powder XRD and Raman etc. were employed to confirm their structural compositions. The halometallates of Fe(III) salt showed elimination of physisorbed water around 100 °C in thermogravimetric analysis as compared to strongly bound water at 150-170 °C in highly crystalline state of the Ni(II) & Co(II) salts. UV-Visible spectra of 4-nitroaniline in aqueous solutions of the chlorometallates gave the Brønsted acidity of the materials. To establish the Lewis acidity, FT-IR spectra of these salts were recorded in presence of pyridine as probe molecule. Catalytic efficiencies of the recyclable chlorometallate salts were explored in one-pot three-component synthesis of 1,2-dihydroquinazolines. The plausible mechanism showed synergistic effects of both Brønsted and Lewis acidic sites in the halometallate catalyst for the enhanced acidity to carry out the reaction.

2.1. Introduction

Organic-inorganic hybrid compounds represent an opportunity for developing new materials with synergic behaviour leading to improved performances of each individual component while reducing their limitations. Halometallates are organic-inorganic hybrid salts, which exist in solid or molten state depending on the strength of electrostatic interactions between organic cations and complex metal halide anions [1, 2]. They may possess interesting properties of metal halide anions such as strong Lewis acidity [3-6], paramagnetism [7], characteristic thermal stability [8], semiconductor behaviour [9] and novel electrochemical properties [10] etc. These metal based organic salts can also hold specific physical/chemical properties including electrical or optical characteristics, electrochemical behaviour and chemical reactivity of functional groups present in the organic cation [1, 11]. Additionally, the organic cations can contribute to the significant hydrophobic/hydrophilic nature of halometallates and their solubility in different solvents. These halometallates have been studied in electrochemistry, catalysis, separation processes, as soft materials and in biomass conversion process based on their tunable physicochemical properties [1]. Most development of halometallates that have been observed till date centred on monocationic organic-inorganic hybrid salts with unique properties of the respective organic cations/metal halide anions [12], specially

catalytic uses of the Brønsted/Lewis acidic chlorometallate salts which are previously reported. In this context, Gogoi *et al.* studied Brønsted-Lewis acidic 3-methyl-1-sulfoimidazolium transition metal chlorides [Msim][X], where X=$[FeCl_4]^-$, $[ZnCl_3]^-$, $[CuCl_2]^-$, as reusable solid acidic catalysts for preparation of *bis*(indolyl)methanes [12]. Saikia *et al.* also prepared another series of 1,3-disulfoimidazolium transition metal chlorides $[Dsim]_2[ZnCl_4]$, $[Dsim][FeCl_4]$ and $[Dsim]_2[NiCl_4]$ as heterogeneous acidic catalysts for one-pot three-component synthesis of β-amino carbonyl compound *via* Mannich type reaction [9]. The formation and catalytic uses of two diethyldisulfoammonium chlorometallates with compositions $[DEDSA][FeCl_4]$ and $[DEDSA]_2[Zn_2Cl_6]$ were introduced by Dutta and group in 2017 [13]. The same author also reported N,N-disulfo-1,1,3,3-tetramethylguanidinium chlorometallates $[DSTMG]_n[X]$, where n=1 or 2; X=$[FeCl_4]^-$, $[Zn_2Cl_6]^{2-}$, $[NiCl_4]^{2-}$, $[MnCl_4]^{2-}$ as reusable acidic catalysts for multi-component synthesis of 1,2-dihydro-1-aryl-3H-naphth[1,2-e][1,3]oxazin-3-ones [14].

The transition of monocationic to dicationic hybrid salts with similar ion-pair offers variations of associated physicochemical behaviour of the dicationic hybrid salts due to diversified compositions of the organic cations, anions and bridging groups in between the cations [15, 16]. For example, the development of inbuilt dicationic Brønsted acidic room temperature organic salts was found based on N,N,N′,N′-tetrasulfopiperazinium cation containing four sulfonic groups ($[TSPi][X]_2$), in combination with three counter anions namely Cl^-, $CF_3SO_3^-$ and TsO^- and investigated their catalytic activities for one-pot sequential synthesis of 2-amino-4,6-diarylpyrimidines under solvet-free conditions *via* Biginelli like reaction [17]. Interestingly, the attachment of two sulfonic groups to each N atom of the dicationic N,N′-disulfopiperazinium dichloride was reported as solid acidic compound (Mp. 220 °C) [18]. By considering the literature of piperazinium based sulfonic acid functionalized organic salts with inherent bridging ability between the organic cations, it was focused to design a new type of dicationic Brønsted-Lewis acidic organic-inorganic hybrids of N,N′-disulfopiperazinium cation [DSPZ][Y] in pairs with three different counter anions of transition metal halides, Y= $[FeCl_4]^-$, $[NiCl_4]^{2-}/[NiCl_3]^-$, $[CoCl_4]^{2-}/[CoCl_3]^-$ (**Scheme 2.1**). Then, the structures of the halometallate organic salts were determined using different analytical techniques and their catalytic efficiencies were studied as recyclable heterogeneous catalysts for three component reaction of 2-amino benzophenone, aromatic aldehydes and ammonium acetate to synthesize 1,2-dihydroquinazolines under

solvent-free conditions and also in solution at varied temperatures (**Scheme 2.2**). Since, many quinazoline derivatives have been known as prospective drugs molecules with broad range of biological activities including anticancer, antibacterial, antimalarial, anti-inflammatory, antifungal agents etc [19-22]. Consequently, the vast attention towards this class of compounds having fused heterocyclic rings has elevated their therapeutic relevance and increased the need for effortless generations of quinazolines. The literature of quinazoline derivatives in **Chapter 1A, sub-unit 1A.4.1** briefly discussed several synthetic methods of these compounds involving Cu-catalysed reactions [23-25], photochemical method [26], tandem reaction of 2-aminobenzophenones and benzylic amines [27, 28], oxidative condensation reactions [29, 30], microwave assisted reactions [31, 32] and so on. These reactions showed various catalytic routes of multicomponent synthesis of quinazolines and 1,2-dihydroquinazolines using acetic acid [33] transition metal catalysts [34, 35], TBBDA [36], Fe_2O_3 supported catalysts [37] and also functionalized ionic liquids such as 1-methylimidazolium triflouroacetate ([Hmim]TFA) [38], butylmethylimidazolium tetrachloroferrate (bmim[$FeCl_4$]) [39], nano-magnetic piperidinium benzene-1,3-disulfonate salt (PBDS-SCMNPs), and triethanolammonium-2,2,2-trichloroacetate (TEATCA) [40]. Only, limited reports are available for the preparation of 1,2-dihydroquinazolines [41-44]. For instance, Kamal *et al.* in 2019 efficiently utilized sulfamic acid as reusable catalyst for preparation of varied 1,2-dihydroquinazolines in ethanol at 60 °C for 20-45 min [45]. Till date, no Brønsted-Lewis acidic halometallate salt was used as catalyst for the synthesis of 1,2-dihydro-2,4-diphenyl quinazolines, as far as we are aware.

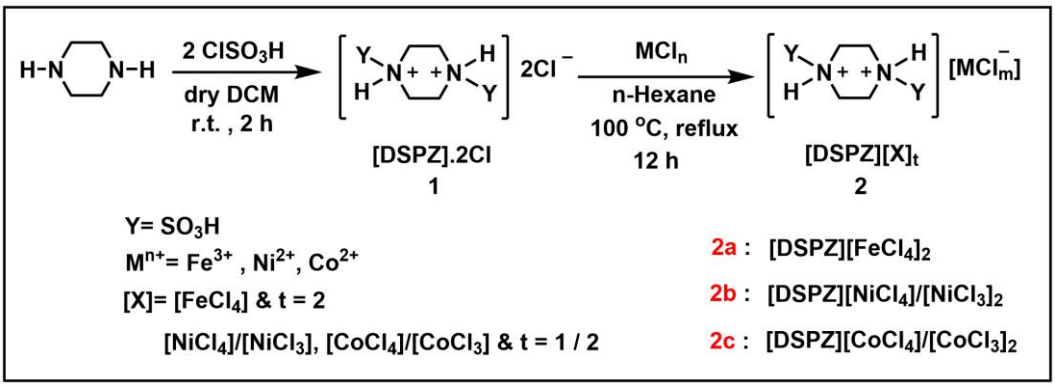

Scheme 2.1: Synthesis of dicationic halometallate hybrids of piperazinium cations.

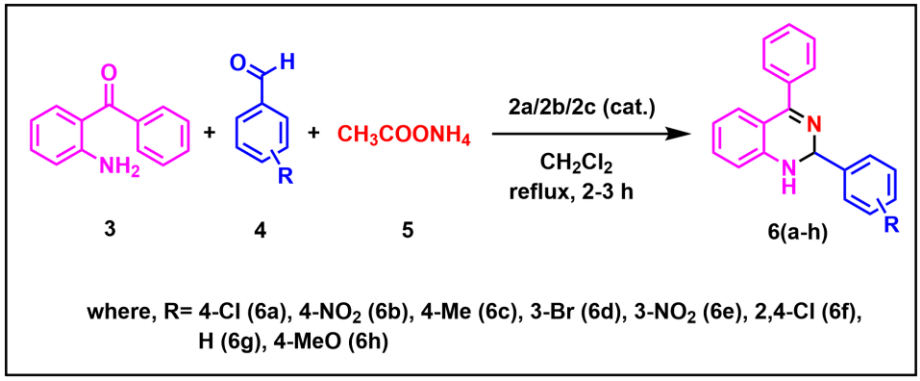

Scheme 2.2: Synthesis of 1,2-dihydroquinazoline products via a three-component reaction.

2.2. Results and discussion

2.2.1. Characterization of halometallate salts

Initially, the synthesis of halometallates of complex anionic speciation of Fe(III), Ni(II) and Co(II) cations with N,N′-disulfopiperazinium cation was done (**Scheme 2.1**) as solid acidic materials by treatment of N,N′-disulfopiperazinium dichloride as obtained from first step with the respective transition metal chlorides in varied mole fractions. Their structural compositions were investigated using FT-IR, UV-Vis diffuse reflectance spectra (DRS), powder-XRD, Raman, SEM, EDX analyses. Thermogravimetric analysis was used to get information about the thermal stabilities and also hydrophilic/hydrophobic properties of the organic salts. Their comparative Brønsted and Lewis acidic strengths were studied by measuring Hammett acidity function H° using UV-visible spectra of 4-nitroaniline in water in presence of the organic salts and FT-IR spectra using pyridine as probe molecule, respectively. Then, their catalytic activities were studied as heterogeneous catalysts for the synthesis of 1,2-dihydroquinazoline derivatives (**Scheme 2.2**) in various organic solvents and also in solvent-free medium at different temperatures.

2.2.1.1. FT-IR and NMR study

The solubility problem of these organic salts in NMR solvents (such as $CDCl_3$, DMSO-d_6, CD_3OD and D_2O) restricted to get information about the organic cation. But, the presence of N,N′-disulfopiperazinium dichloride cation in these salts can be supported indirectly from ^1H and ^{13}C NMR spectra (**section 2.4.6**) of the parent organic

salt, N,N′-disulfopiperazinium dichloride ([DSPZ].2Cl) and also their comparative FT-IR spectra (**Fig. 2.1a** & **section 2.4.6**) [18]. The ^{1}H NMR spectrum of [DSPZ].2Cl salt displayed one singlet at δ 9.32 ppm for two sulfonic acid protons, broad singlet at δ 6.58 ppm for two N-H protons and a sharp singlet of eight methylene protons at δ 3.29 ppm. The ^{13}C NMR spectrum showed only one peak, which can be attributed to four equivalent C atoms of piperazine ring.

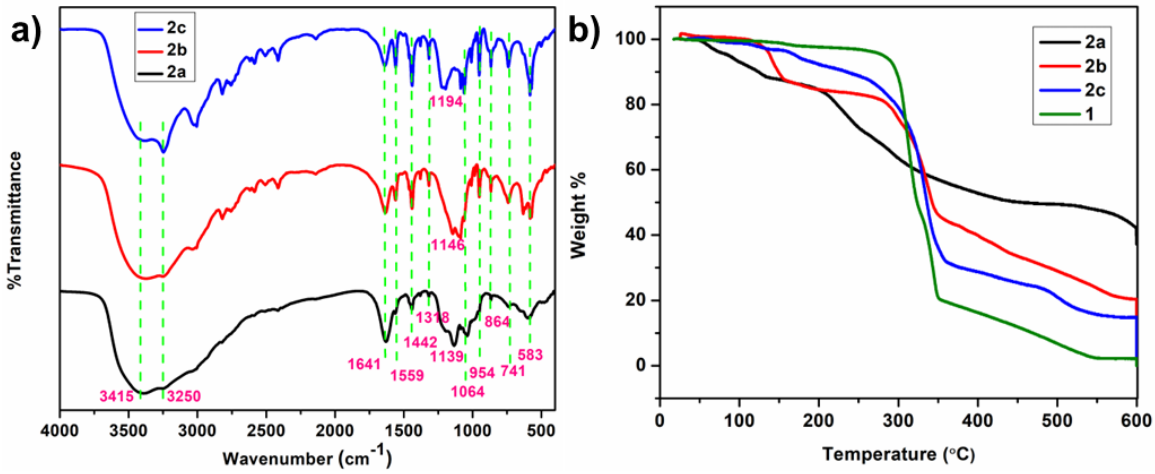

Fig. 2.1: a) FT-IR spectra of **2a**, **2b** and **2c** organic salts, b) TGA plots of piperazinium based organic salts.

Assignments of various absorption frequencies of the three chlorometallates were done by correlating their FT-IR spectra (**Fig. 2.1a**) with that of the reported chloride salt (**section 2.4.6**). The three halometallates possess characteristic vibrations of -SO_3H group by displaying strong absorption peaks at 1064 cm^{-1} for S-O symmetric stretch, 1139-1194 cm^{-1} for antisymmetric stretch and 583 cm^{-1} for bending vibration like the parent chloride salt. The two peaks at 864 cm^{-1} and 1318 cm^{-1} could be assigned for N-S and C-N stretches, respectively. Peaks at 741 cm^{-1} and 1442 cm^{-1} appeared because of out of plane ring bending of C-H bond and bending vibrations of CH_2 groups present in piperazine ring. Bending vibration of N-H bond was confirmed by peak at 1641 cm^{-1}. Presence of broad peaks around 2700-3500 cm^{-1} could be attributed for overlapped N-H bond stretch, O-H bond stretch of -SO_3H groups involving intermolecular H-bonded water molecules and also C-H bond stretching vibrations.

2.2.1.2. Thermogravimetric analysis (TGA)

Fig. 2.1b displayed comparative TGA plots of the chlorometallates of N,N′-disulfopiperazinium cation with their parent chloride salt [DSPZ].2Cl. Like the chloride salt, the Ni(II) and Co(II) organic salts did not show any loss of physisorbed water around 100 °C in contrast to elimination of around 12% of moisture in case of the Fe(III) organic salt and thus Fe(III) salt could be expressed as the most hydrophilic salt. The next weight loss of Fe(III) salt was observed around 220 °C with slow degradation of N,N′-disulfopiperazinium cation to retain the metal salt residue. The TGA plots of Ni(II) and Co(II) salts showed two step decompositions where 5-10% weight loss observed in 1st step around 150-170 °C followed by 2nd step decomposition at 280-300 °C. The 1st step mass loss could be accounted for slow release of 5-10% of captured crystalline water above 100 °C [46], which was evidenced from their highly crystalline SEM images (**Fig. 2.3b-c**) for the Ni(II) and Co(II) salts.

2.2.1.3. UV-Vis diffuse reflectance spectra

The three different halometallate anions of N,N′-disulfopiperazinium cation showed different absorption peaks in UV-DRS spectra as shown in **Fig. 2.2a**. For Fe(III) salt (**2a)**, absorbance peaks at 243 nm and 435 nm could be assigned as ligand to metal charge (L→Fe(+3)) transfer transitions [47, 48]. In addition to that, $^{6}A_1 \rightarrow {}^{4}A_2$ transition was observed at 602 nm which was a typical absorption for $FeCl_4^-$ anion [49]. The electronic spectra of Ni(II) salt (**2b**) displayed two absorbance peaks at 721 nm and 784 nm corresponding to $^{3}T_1(F) \rightarrow {}^{3}T_1(P)$ (ν_3) spin-allowed transition of Ni^{2+} in tetrahedral configuration [50-53]. Peak position at 430 nm could be assigned as $^{3}A_{2g}(F) \rightarrow {}^{3}T_{1g}(P)$ transition of small amount of octahedral Ni(II) complex [50, 54] with red shift of peak position for partial replacement of water ligand by Cl^- which might be present in equilibrium with predominant amount of tetrahedral Ni(II) chloride anion $NiCl_4^{2-}$ in addition to a small amount of hydrated tetrahedral chloro species as $[NiCl_3(H_2O)]^-$ as observed from the weak shoulder around 510 nm of $NiCl_3^-$ anion [55-57]. The peak at 221 nm could be assigned for L→M charge transfer transition for tetrahedral complexes based upon ligand field theory. These analyses support that the most probable anionic composition of Ni(II) salt must exist in equilibrium speciations of $NiCl_3^-$ /$NiCl_4^{2-}$ anions with distorted tetrahedral structure of $NiCl_4^{2-}$ which could be inactive in Raman analysis and hence expected in the Raman analysis of Ni(II) salt.

Similarly, the spectra of Co(II) salt (**2c**) showed one broad absorption in the range of 600-700 nm, corresponding to triplet peak of tetrahedral $[CoCl_4]^{2-}$ speciation with absorption maximum around 622 nm, 671 nm and 698 nm. These triplet peaks observed for $^4T_1(P) \rightarrow {}^4A_2(F)$ transition imparted a strong blue color to the halometallate of Co(II), which evidenced the existence of $[CoCl_4]^{2-}$ as dominant species [51, 58]. The small shoulder at 529 nm showed existence of small amount of $CoCl_3^-$ species in equilibrium with the $CoCl_4^{2-}$ [59]. A small peak at 450 nm could be attributed for mixing of small amount of hydrated octahedral complex of Co^{2+} cation [60]. The peak around 244 nm could be considered for ligand to metal charge transfer transition of tetrahedral $[CoCl_4]^{2-}$ based on ligand field theory. Thus, the electronic spectra of Co(II) salt displayed its most possible anionic composition of chlorometallates as an equilibrium mixture of $CoCl_4^{2-}$ & $CoCl_3^-$ [53] with distorted tetrahedral structure of $CoCl_4^{2-}$ and this could be inactive in the Raman analysis like the Ni(II) salt. Due to weak coordination power and lower dielectric constant of tetrahedral $[CoCl_4]^{2-}$ species than $CoCl_2$, it preferably absorbs UV light at a longer wavelength than other coordination-unsaturated cobalt-chloro complex clusters.

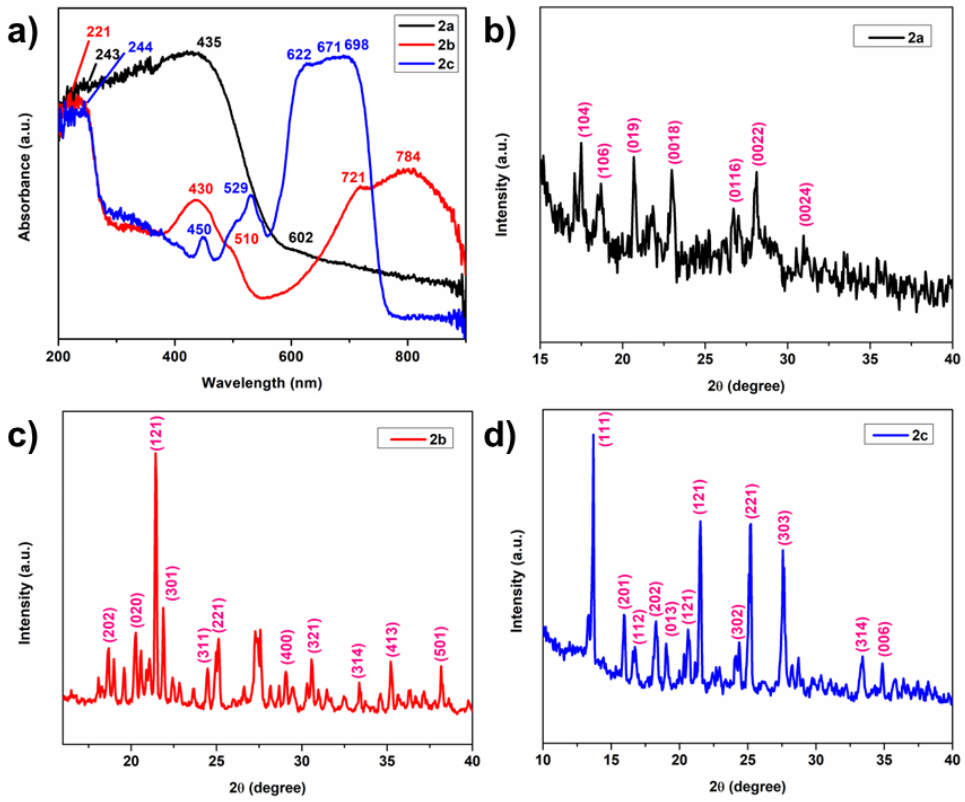

Fig. 2.2: a) UV-DRS spectra of **2a**, **2b** and **2c** organic salts, b-d) PXRD patterns of **2a**, **2b** and **2c** salts.

2.2.1.4. Powder X-ray diffraction analysis

The powder-XRD patterns of chlorometallates in **Fig. 2.2b-d** showed characteristic 2θ peaks of respective transition metal chlorides. In case of Fe(III) hybrid **2a**, the sharp peaks at 2θ=17.48°, 18.68°, 20.68°, 22.97° and 28.07° decently matched the XRD database of $FeCl_3$ (JCPDS card no. 77-0999) indicating reflection planes (104), (106), (019), (0018) and (0022), respectively. Similarly, the 2θ values at 18.68°, 19.58°, 21.43°, 22.47°, 24.97°, 25.12°, 29.07°, 30.56° and 35.21° were observed for **2b**, which resembled satisfactorily with $[N(CH_3)_4]_2.NiCl_4$ (JCPDS card no. 72-0034) corresponding to (202), (020), (121), (301), (311), (221), (400), (321) and (431) reflection planes. Likewise, the organic salt **2c** displayed peaks at 2θ=13.68°, 15.93°, 16.58°, 18.29°, 19.03°, 20.63°, 21.52°, 24.37°, 25.22°, 27.57°, 33.41° and 34.86° with reflection planes of (111), (201), (112), (202), (020), (113), (121), (311), (221), (303), (314) and (006) planes, which was found to be quite similar to the XRD databases of $[N(CH_3)_4]_2.CoCl_4$ (JCPDS card no. 72-0033).

2.2.1.5. Scanning Electron Microscopy analysis

The representative SEM images of three dicationic piperazinium halometallates of transition metal chlorides, as shown in **Fig. 2.3a-c**, expressed variations of surface morphology of crystallite particles which might be expected for different amount of crystallized and physisorbed water present in equilibrium with tetrahedral complex of metal chlorides [55]. The image of **2a** portrayed irregular surface distribution of small crystallite sizes as well as few numbers of micro-granular structures. Both the SEM images of **2b** and **2c** displayed distribution of medium to larger sized crystalline structures and also their aggregated form on their surfaces. The existence of captured water within these crystalline structures could be evidenced from the TGA plots for release of around 5-10% of moisture content for these two salts above 100 °C before 2^{nd} degradation temperature at 280 °C.

2.2.1.6. EDX analysis

Energy dispersive X-ray (EDX) analysis as shown in **Fig. 2.3d-f** confirmed the presence of respective metal chlorides as well as other constituent elements of N,N′-disulfopiperazinium halometallates. No impurities or undesired elements were found in any of the compounds.

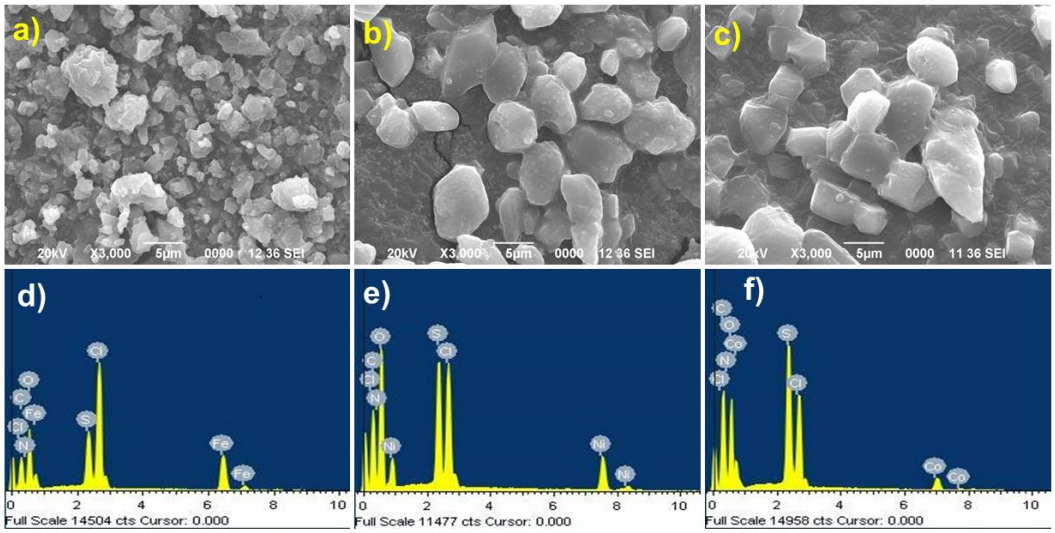

Fig. 2.3: a-c) SEM images, d-f) EDX images of **2a**, **2b** and **2c** organic salts.

2.2.1.7. Raman analysis

In the Raman spectrum of **2a**, strong peaks at 112 cm^{-1} and 335 cm^{-1} could be seen, as shown in **Fig. 2.4**. These two peaks could be assigned as bending modes of Cl-Fe-Cl ($\nu_2(E)$) and stretching modes of Fe-Cl bond ($\nu_1(A_1)$), respectively [61]. The tetrahedral chloride anions of Ni(II) and Co(II) organic salts were found to be Raman inactive as expected from their electronic spectra and thus supported the existence of distorted tetrahedral structures of $NiCl_4^{2-}$ & $CoCl_4^{2-}$ due to mixed compositions with the $NiCl_3^-$ & $CoCl_3^-$, respectively, in hydrated environment as expressed in the electronic spectra (**Fig. 2.2a**). So, their anionic composition could be represented as a mixture of $NiCl_3^-/NiCl_4^{2-}$ and $CoCl_3^-/CoCl_4^{2-}$.

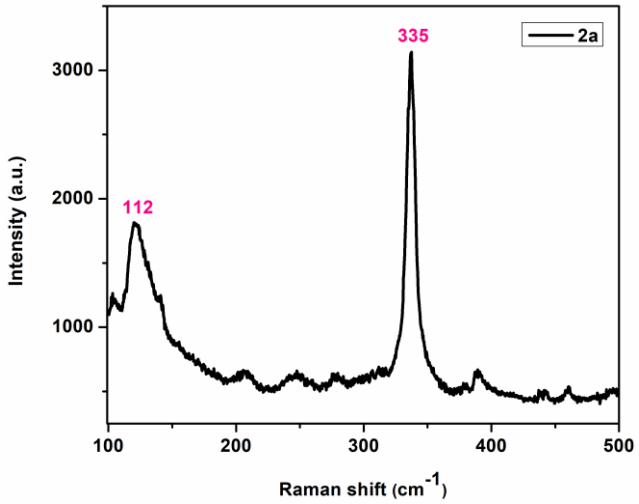

Fig. 2.4: Raman spectrum of **2a.**

2.2.1.8. Hammett acidity measurement

The strength of Brønsted acidity sites of these materials was determined through comparative UV-visible spectra of 4-nitroaniline in water containing the three halometallates as well as the parent ionic salt (**Fig. 2.5**) in descending order as calculated from Hammett acidity function H^o values (**Table 2.1**) using **Equation (1B.1) (Chapter 1B, sub-section 1B.3.8)** according to standard literature method [62, 63], where 4-nitroaniline was employed as a basic indicator to determine the acidity of organic salts.

$$H^o = pK(I)_{aq} + \log[I]/[IH]^+ \qquad \textbf{Equation (1B.1)}$$

Here $pK(I)_{aq}$ represents pKa value of the basic indicator in aqueous solution.

Treatment of equimolar amount of 4-nitroaniline (pKa = 0.99) and catalyst (5 mmol/L) in distilled water solution was used to check the absorbance by the organic salts. The indicator showed maximum absorbance at 379 nm in distilled water. With increasing acidity of the organic salts, the absorbance of indicator [I] in organic salt solutions reduced. Thus, the descending Brønsted acidity order of organic metal chlorides against their H^o values was found as : 2a > 2c > 2b, where the Fe(III) salt showed strong Brønsted acidic character with its minimum Hammett acidity value.

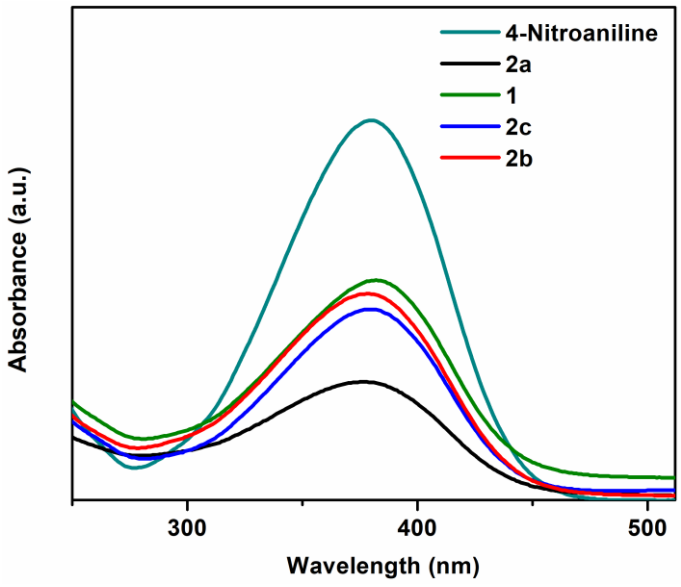

Fig. 2.5: Comparative UV-visible spectra of 4-nitroaniline in water containing halometallates (**2a**, **2b** & **2c)** and parent chloride salt **1**.

Table 2.1: Measurement of Hammett function using **Equation 1B.1**.

Entry	Name	Absorbance	[I]%	[HI]%	H_o
1	4-Nitroaniline	0.6160	100	0	-
2	[DSPZ].2Cl	0.3555	57.57	42.29	1.125
3	2a	0.1929	31.31	68.69	0.649
4	2b	0.334	54.22	45.78	1.063
5	2c	0.3085	50.08	49.92	0.991

2.2.1.9. Lewis acidity study

The presence of Lewis acidic sites and their comparative acidic strength for the prepared halometallates were supported by FT-IR analysis of adsorbed pyridine as probe molecule with variation of absorption band differences at 1545 cm^{-1} and 1455 cm^{-1}, corresponding to Brønsted acidic pyridinium ion and pyridine coordinated Lewis acidic sites, respectively [64-66]. Accordingly, the peak at 1438 cm^{-1}, as shown in **Fig. 2.6**, by neat pyridine was found to be relocated towards higher wavenumber when pyridine complexed with these salts i.e., 1449 cm^{-1} for Fe(III) salt (**2a**), 1447 cm^{-1} for Ni(II) salt (**2b**) and 1445 cm^{-1} for Co(II) salt (**2c**), respectively. Their Lewis acidic strengths were found to be slightly varied as observed from the absorption frequencies. Among them, the Fe(III) salt expressed more Lewis acidic strength. The quatitative measurement of Lewis acidic site was not feasible due to lack of precise molar extinction coefficient [67, 68]. Additionally, the appearance of another peak at 1539 cm^{-1} for all the organic salts evidenced the existence of Brønsted acidic sites. For catalytic uses of these Brønsted-Lewis acidic materials, we could expect synergistic effect of the Brønsted-Lewis acidic sites to work as efficient heterogeneous catalysts in organic reactions [69].

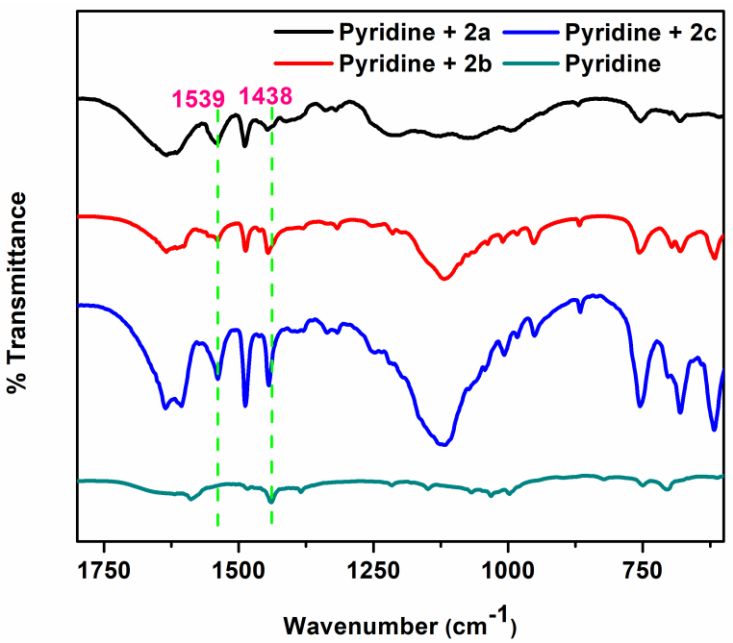

Fig. 2.6: Lewis acidity check for the halometallate ionic salts by comparative FT-IR spectroscopy.

2.2.2. Catalytic study

2.2.2.1. Optimization of reaction conditions

The catalytic efficiencies of three chlorometallates **2a-c**, were explored by conducting the one-pot three-component reaction of 2-aminobenzophenone (1 mmol), 4-chlorobenzaldehyde (1 mmol) and ammonium acetate (~1.5 mmol) as model reaction in CH_2Cl_2 (DCM) for preparation of substituted 1,2-dihydroquinazolines (**Scheme 2.2**) with varied amount of the catalysts (5, 10 and 15 mol%) at ambient and reflux temperatures as mentioned in **Table 2.2**.

Table 2.2: Optimization of reaction conditions for synthesis of 1,2-dihydroquinazoline product (**6a**).

Entry	Catalyst	Catalyst amount (mol%)	Temperature (°C)	Time (h) [b]	%yield[a](**6a**)
1	-	-	Reflux	3	Trace
2	**2a**	**5/10/15**	**Reflux**	**2.25**	**82/87/87**

3	2a	5/10/15	25	2.25	62/68/70
4	2b	10	Reflux	2.83	82
5	2b	10	25	2.83	62
6	2c	10	Reflux	2.50	85
7	2c	10	25	2.50	67

[a] Isolated yield; [b] reactions run in CH_2Cl_2

It was noticed that increasing amount of the catalyst increased the isolated yields of products, where little differences in product yields were observed for the 10 mol% and 15 mol% of **2a** catalyst in these reaction conditions. Therefore, only 10 mol% of **2b** and **2c** was utilized to check the reaction outcomes. However, only trace amount of the product **6a** was formed in absence of the catalyst (**Table 2.2, entry 1**). Again, the yields of products under reflux temperature in DCM were higher than those at ambient temperature (**Table 2.2, entries 2, 4, 6**). The model reaction showed better yields of products in lesser reaction time for Fe(III) salt, hence 10 mol% of Fe(III) salt was selected as the Brønsted-Lewis acidic material for solvent effect study. These results also supported the lesser acidic strength of the Ni(II) and Co(II) organic salts, as compared to that of Fe(III) salt. The solvent effect for the model reaction using 10 mol% of the Fe(III) salt was also studied under reflux temperature in polar and non-polar solvents including water, acetonitrile, ethanol, ethyl acetate as well as in solvent-free grinding method at room temperature. The yields were not satisfactory for water medium (**Table 2.3, entry 4**), whereas acetonitrile (**Table 2.3, entry 5**), ethanol (**Table 2.3, entry 6**) and ethyl acetate (**Table 2.3, entry 7**) mediated reactions showed decent results. Also, solvent-free grinding method at room temperature generated lesser amount of product yield (**Table 2.3, entry 3**). The outcome of the solvent effect study expressed CH_2Cl_2 under reflux condition as the best solvent-system for these three-component reactions to carry out (**Table 2.3, entry 2**). By considering these observations, it was decided to proceed with the substrate scope study for other aromatic aldehydes containing electron-withdrawing or donating groups in CH_2Cl_2 under reflux temperature in presence of 10 mol% of the Fe(III) catalyst (**2a**) as standard reaction conditions for this three-component reaction.

Table 2.3: Solvent effect study on the model compound **6a** for 10 mol% of catalyst **2a**.

Entry	Solvent	Temperature (°C)	Time (h)	% yield[a] (**6a**)
1	CH_2Cl_2	25	2.25	68
2	**CH_2Cl_2**	**40**	**2.25**	**87**
3	solvent-free	25	1	38
4	H_2O	100	5	29
5	CH_3CN	82	3	77
6	EtOH	78	3	68
7	EtOAc	77	3	71

[a] Isolated yield

2.2.2.2. Substrate scope study for the synthesis of 1,2-dihydroquinazoline products

Under the optimized conditions, various 1,2-dihydroquinazoline products (**6a-h**) were synthesized by the three component reactions of 2-aminobenzophenone and ammonium acetate with several substituted aromatic aldehydes. The results portrayed that aldehydes with electron-withdrawing substituents resulted in slightly better yields of products in lesser reaction time, as shown in **Scheme 2.3**.

A comparative study was performed between the present work and earlier reports, as shown in **Table 2.4**, which displayed mild reaction conditions as well as use of minimum amount of the catalyst to generate modest yield of the desired products.

Table 2.4: A comparison of the present work with earlier reports of 1,2-dihydroquinazoline derivatives synthesis.

Entry	Catalyst	Solvent	Temp. (°C)	Time	%Yield [Ref.]
1	-	[emim][PF_6]/PhMe Or	160[a]	30 min	72-94 [41]

		[emim][PF_6]/*t*-BuOH			
2	-	-	130[b]	4 min	78-90 [42]
3	4-(N,N-dimethylamino) pyridine (DMAP) (20 mol%)	EtOH	40	1-2 h	67-98 [43]
4	-	EtOH	60	2 h	66-91 [44]
5	Sulfamic acid (20 mol%)	EtOH	60	20-45 min	81-96 [45]
6	[DSPZ][$FeCl_4$]$_2$ (10 mol%)	CH_2Cl_2	40	2-3 h	74-89 [This work]

[a] Under microwave (MW) irradiation (300 MHz); [b] Under MW irradiation (540 W).

2.2.2.3. Plausible mechanism

The plausible mechanism of **2a** catalyzed three-component synthesis of 1,2-hydroquinazolines (**6a**) could be proposed through synergistic effects of both Brønsted-Lewis acidic sites in the halometallate catalyst for activation of carbonyl group as well as ammonia, generated from ammonium acetate, for nucleophilic attack as represented in **Scheme 2.4.**

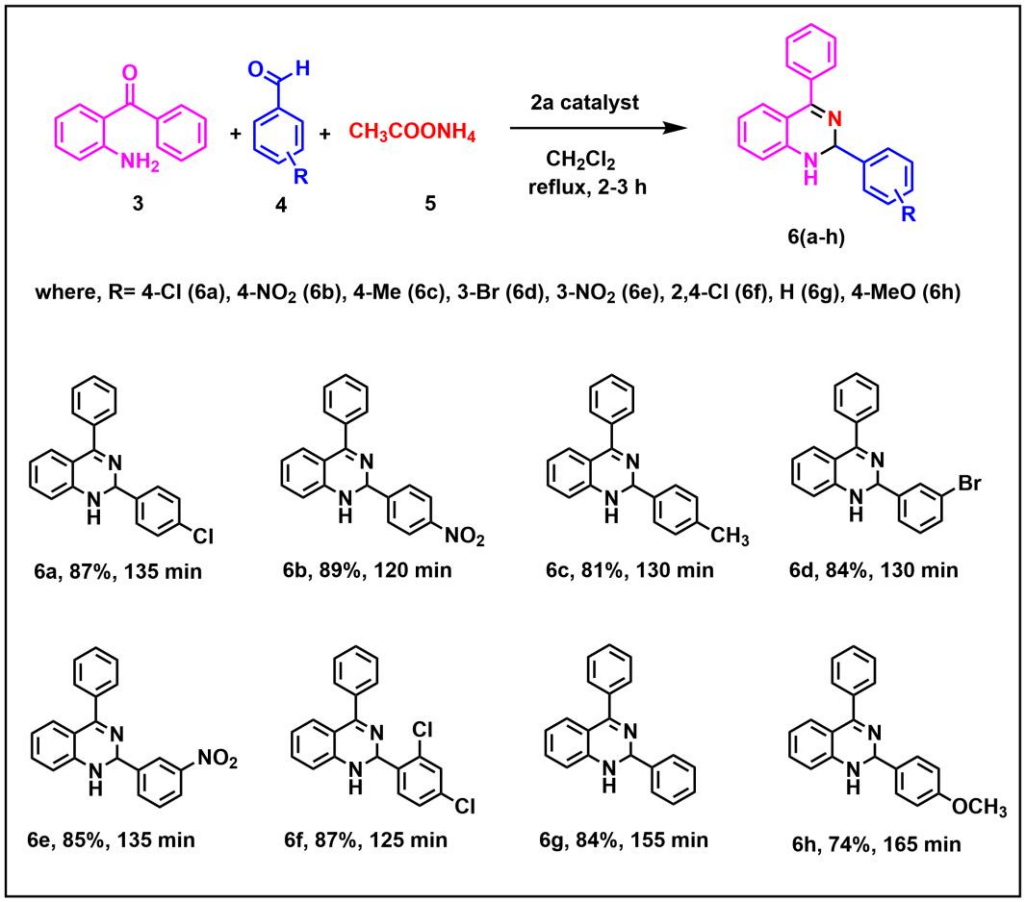

Scheme 2.3. Substrate scope study with aromatic aldehydes for the synthesis of 1,2-hydroquinazolines using 10 mol% of **2a** as catalyst in 5 mL DCM.

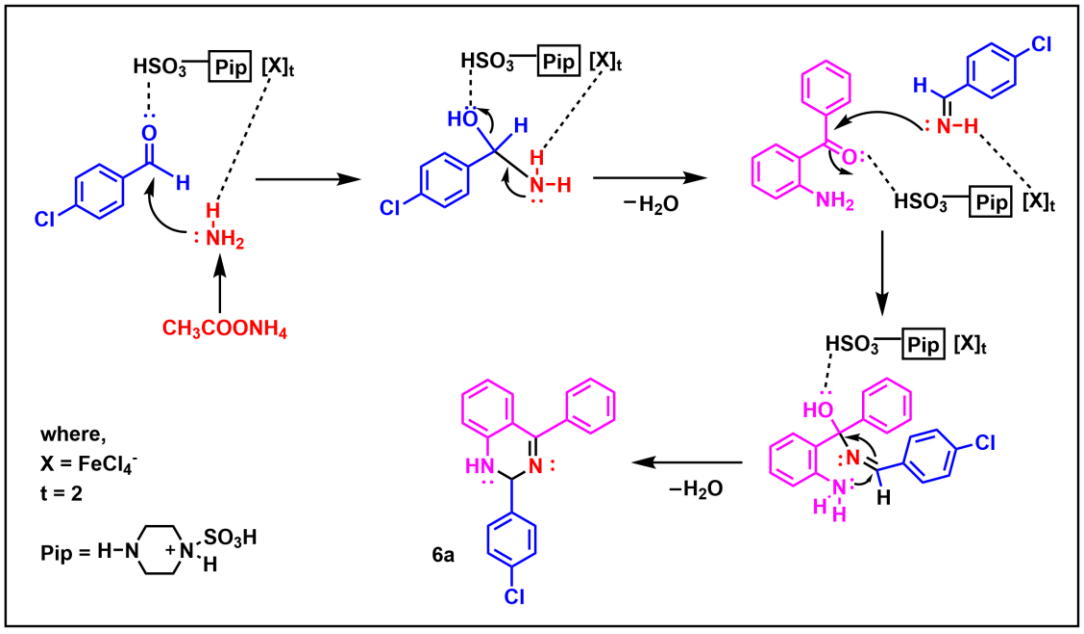

Scheme 2.4: Plausible reaction mechanism for the synthesis of 1,2-dihydroquinazoline products.

2.2.3. Catalyst recyclability

The reusability of used catalyst **2a** was checked with the model reaction in 3 mmol scale for three runs, as shown in **Fig. 2.7a**, which was further evidenced from characteristic FT-IR spectrum of 3rd time recycled catalyst with the fresh Fe(III) salt (**Fig. 2.7b**). The recycling of catalyst was done after filtration of the reaction mixture in DCM solution which retained the catalyst as solid residue. The residue was then washed with 5 ml of DCM for 3 times, dried in vacuum oven at 50 °C and used in the next cycle. **Fig. 2.7a** depicted moderate decrease of product yield **6a** after each consecutive cycle for the same reaction period, which could be attributed for repeated washing of the used catalyst and then reactivation in vacuum that might reduce the activity of acidic sites present on the heterogeneous catalyst.

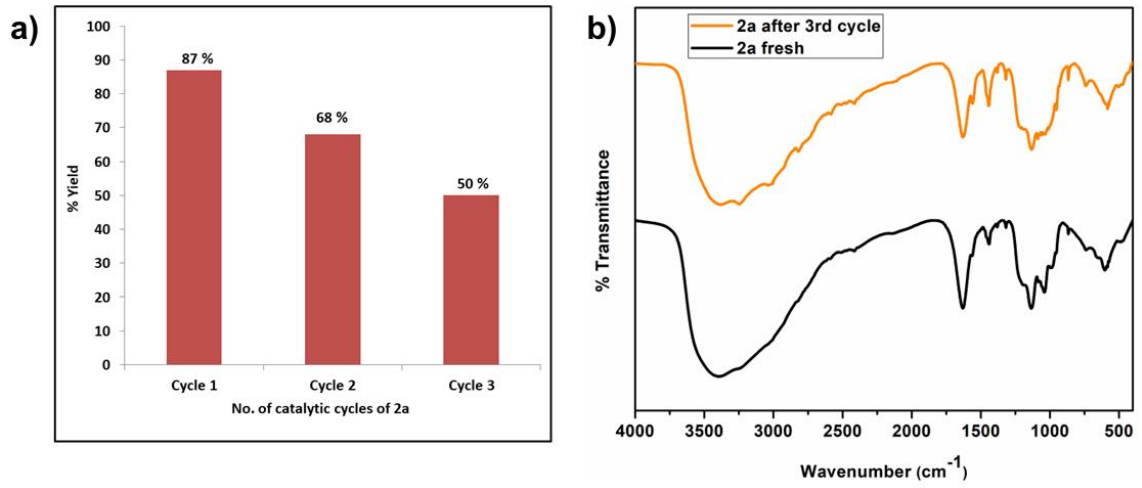

Fig. 2.7: a) Recyclability profile for the model reaction showing %yield of **6a** with catalyst **2a** at 2.25 h of reaction time, b) FT-IR spectra of catalyst **2a** freshly prepared and after 3rd cycle.

2.3. Summary

In summary, we have developed three organic salts of complex metal chloride anions of Fe(III), Ni(II) and Co(II) cations with N,N′-disulfopiperazinium cation as solid Brønsted-Lewis acidic materials. They were fully characterized through various analytical and spectroscopic techniques including FT-IR, TGA, UV-DRS, SEM, EDX, powder-XRD and Raman techniques. Their catalytic efficiencies were also explored in synthesizing 1,2-dihydroquinazoline derivatives through one-pot three-component reactions of 2-aminobenzophenone, substituted aromatic aldehydes and ammonium

acetate. Under the optimized conditions, the reaction showed best results for 10 mol% of Fe(III) salt in DCM with aldehydes having electron-withdrawing groups. The acidic organic salts acted as heterogenous catalysts in the reactions and were easy to recover, facilitating their recyclable nature for further reactions.

2.4. Experimetal Section

2.4.1. Synthesis of N,N′-disulfopiperazinium chloride ([DSPZ].2Cl) (1) and N,N′-disulfopiperazinium halometallates (2a, 2b, 2c)

The preparation of three halometallates of N,N′-disulfopiperazinium cation was comprised of two steps method (**Scheme 2.1**). The parent N,N′-disulfopiperazinium chloride ([DSPZ].2Cl) (**1**) was isolated as a white solid in 1st step of the reaction, according to standard procedure, through treatment of 5 mmol of piperazine in dry dichloromethane (30 mL) with HSO_3Cl (10 mmol) at room temperature for 2 hours [18]. In the next step, the respective transition metal chlorides of Fe(III), Ni(II) and Co(II) were mixed in varied mole fractions i.e. χ ($FeCl_3$) = 0.67, χ ($NiCl_2{\cdot}6H_2O$) = 0.5 and χ ($CoCl_2{\cdot}6H_2O$) = 0.5, respectively, with the parent N,N′-disulfopiperazinium chloride ([DSPZ].2Cl) (**1**) (5 mmol) in n-hexane as reaction medium. The mixtures were treated under reflux condition with continuous stirring in oil bath for 12 hours at 100 °C. After that, the mixtures were cooled to room temperature and then filtered to get the halometallates as solid residues, which were washed two times with CH_2Cl_2 for removal of soluble impurities. The three organic salts of halometallates were dried under vacuum for 6 hours at 60 °C and produced 96-97 % yields as dark yellow $[DSPZ][FeCl_4]_2$ (**2a**), yellowish green $[DSPZ][NiCl_4]/[NiCl_3]_2$ (**2b**) and blue coloured $[DSPZ][CoCl_4]/[CoCl_3]_2$ (**2c**) solid materials.

2.4.2. Typical procedure for the synthesis of 1,2-dihydroquinazoline products (6a-h)

In a 50 mL round bottom flask, a mixture of equimolar amounts of 2-aminobenzophenone **3** (1 mmol), aromatic aldehyde **4** (1 mmol) and ammonium acetate **5** (~1.5 mmol) was added to 5 mL of CH_2Cl_2 solvent. The reaction was carried out under reflux in an oil bath for about 2-3 hours with continuous stirring, containing 10 mol% of the organic salts as catalysts, as shown in **Scheme 2.2**. The progress of the reaction was monitored by thin layer chromatography (TLC) technique using EtOAc and petroleum ether (1:5) as mobile phase. At the end of the reaction, the mixture was diluted with more

amount of CH_2Cl_2 (10 mL) and filtered to get the used catalyst from the organic extract for reactivation. The product mixture in CH_2Cl_2 solution was washed with an aqueous solution of $NaHCO_3$ to neutralize the acidic impurities available from the starting aldehydes. The crude product was isolated by evaporating the organic solvent in rotary evaporator and further purified by preparative TLC technique to get analytically pure product. Spectral data, ^1H NMR and ^{13}C NMR spectra of 1,2-dihydroquinazoline products (**6a-h**) are given in **section 2.4.5**, **section 2.4.7** and **section 2.4.8**, respectively.

2.4.3. Spectral data of N,N′-disulfopiperazinium chloride organic salt (1)

1: White solid, 95% yield, FT-IR (KBr) ν cm^{-1} : 3415, 3250, 3009, 1641, 1559, 1442, 1318, 1174, 1064, 941, 864, 741 and 583; ^1H NMR (DMSO-d_6, 400 MHz): δ 9.32 (s, 2H), 6.58 (s, 2H), 3.29 (s, 8H); ^{13}C NMR (DMSO-d_6), 100 MHz): δ 87.35.

2.4.4. Spectral data of N,N′-disulfopiperazinium halometallate organic salts (2a, 2b, 2c)

2a: Dark yellow solid, 97% yield; FT-IR (KBr) ν cm^{-1}: 3415, 3250, 1641, 1442, 1318, 1194, 1064, 864, 741 and 583.
2b: Yellowish green solid, 97% yield; FT-IR (KBr) ν cm^{-1}: 3415, 3250, 1641, 1442, 1318, 1146, 1064, 864, 741 and 583.
2c: Blue solid, 96% yield; FT-IR (KBr) ν cm^{-1}: 3415, 3250, 1641, 1442, 1318, 1139, 1064, 864, 741 and 583.

2.4.5. Spectral data of 1,2-dihydroquinazolines

2-(4-chlorophenyl)-4-phenyl-1,2-dihydroquinazoline [44, 45, 70] (**6a**) : Greenish yellow solid; FT-IR (KBr) ν cm^{-1} : 3390, 3243, 3063, 2924, 2249, 1613, 1561, 1485, 1338, 1095, 907, 691 and 539; ^1H NMR ($CDCl_3$, 400 MHz): δ 7.56-7.51 (m, 4H), 7.44-7.39 (m, 3H), 7.35 (d, *J*=8.0Hz, 2H), 7.25 (t, *J*= 8.0 Hz, 1H), 7.17 (d, *J*=8.0 Hz, 1H), 6.73 (t, *J*=8.0 Hz, 1H), 6.67 (d, *J*=8.0 Hz, 1H), 5.89 (s, 1H), 4.28 (s, 1H); ^{13}C NMR ($CDCl_3$, 100 MHz): δ 166.12, 146.69, 141.12, 138.01, 134.20, 129.28, 128.91, 128.82, 128.29, 118.58, 117.95, 114.45, 100.00, 71.96; CHN analysis (Mol. Formula $C_{20}H_{15}ClN_2$): calculated (%) C 75.35, H 4.74, N 8.79; Found (%) C 75.32, H 4.72, N 8.73.

2-(4-nitrophenyl)-4-phenyl-1,2-dihydroquinazoline [44, 45, 70] **(6b)** : Yellow solid; FT-IR (KBr) ν cm^{-1} : 3400, 2921, 2249, 1618, 1519, 1348, 1080, 850, 750, 699 and 533; ^1H

NMR ($CDCl_3$, 400 MHz): δ 8.22 (d, *J*=8.0 Hz, 2H), 7.78 (d, *J*=8.0 Hz, 2H), 7.55 (d, *J*=8.0 Hz, 2H), 7.45-7.41 (m, 3H), 7.28-7.26 (m, 1H), 7.18 (d, *J*=8.0 Hz, 1H), 6.77-6.71 (m, 2H), 6.04 (s, 1H), 4.38 (s, 1H); ^{13}C NMR ($CDCl_3$, 100 MHz): δ 166.53, 149.50, 147.91, 146.25, 137.76, 129.22, 128.43, 123.94, 118.99, 118.00, 114.68, 71.71; CHN analysis (Mol. Formula $C_{20}H_{15}N_3O_2$): calculated (%) C 72.94, H 4.59, N 12.76; Found (%) C 72.92, H 4.53, N 12.71.

4-phenyl-2-(*p*-tolyl)-1,2-dihydroquinazoline [43] (**6c**) : Yellow solid; FT-IR (KBr) ν cm^{-1} : 3464, 3349, 3065, 2915, 1612, 1541, 1441, 1341, 1164, 1021, 936, 758, 700 and 544; ^1H NMR ($CDCl_3$, 400 MHz): δ 7.57-7.55 (m, 2H), 7.48-7.46 (m, 2H), 7.41-7.39 (m, 3H), 7.23-7.21 (m, 1H), 7.19-7.14 (m, 3H), 6.7 (t, *J*=8.0 Hz, 1H), 6.66 (d, *J*=8.0Hz, 1H), 5.90 (s, 1H), 4.24 (s, 1H), 2.34 (s, 3H); ^{13}C NMR ($CDCl_3$, 100 MHz): δ 165.72, 146.93, 139.72, 138.24, 138.16, 129.42, 129.33, 128.19, 128.17, 127.30, 118.24, 117.96, 114.30, 72.53; CHN analysis (Mol. Formula $C_{21}H_{18}N_2$): calculated (%) C 84.53, H 6.08, N 9.39; Found (%) C 84.51, H 6.02, N 9.30.

2-(3-bromophenyl)-4-phenyl-1,2-dihydroquinazoline **(6d)** : Yellow solid; FT-IR (KBr) ν cm^{-1} : 3436, 2928, 2246, 1630, 1472, 1342, 1249, 1070, 698 and 532; ^1H NMR ($CDCl_3$, 400 MHz): δ 8.14 (t, *J*=8.0 Hz, 1H), 7.92-7.86 (m, 1H), 7.77-7.76 (m, 1H), 7.63-7.59 (m, 2H), 7.55 (m, 1H), 7.44-7.41 (m, 3H), 7.28-7.26 (m, 1H), 7.17 (d, *J*=8.0 Hz, 1H), 6.73 (t, *J*=8.0 Hz, 1H), 6.69 (d, *J*=8.0 Hz, 1H), 5.89 (s, 1H), 4.28 (s, 1H); ^{13}C NMR ($CDCl_3$, 100 MHz): δ 166.23, 146.62, 144.95, 137.97, 133.89, 130.34, 129.29, 128.27, 122.79, 121.94, 118.02, 117.12, 114.45, 72.14; CHN analysis (Mol. Formula $C_{20}H_{15}BrN_2$): calculated (%) C 66.13, H 4.16, N 7.71; Found (%) C 66.08, H 4.13, N 7.66.

2-(3-nitrophenyl)-4-phenyl-1,2-dihydroquinazoline [45, 70] **(6e)** : Yellow solid; FT-IR (KBr) ν cm^{-1} : 3436, 2921, 2254, 1622, 1529, 1464, 1342, 1076, 905, 697 and 532; ^1H NMR ($CDCl_3$, 400 MHz): δ 8.46-8.45 (m, 1H), 8.17 (d, *J*=8.0 Hz, 1H), 7.96-7.95 (m, 1H), 7.62 (m, 1H), 7.56-7.53 (m, 2H), 7.45-7.41 (m, 3H), 7.30-7.28 (m, 1H), 7.18 (d, *J*=8.0 Hz, 1H), 6.77-6.70 (m, 2H), 6.05 (s, 1H), 4.24 (s,1H); ^{13}C NMR ($CDCl_3$, 100 MHz): δ 166.70, 148.43, 146.34, 144.71, 137.67, 133.78, 130.29, 129.47, 128.33, 123.37, 122.55, 118.99, 117.99, 114.73, 71.53; CHN analysis (Mol. Formula $C_{20}H_{15}N_3O_2$): calculated (%) C 72.94, H 4.59, N 12.76; Found (%) C 72.90, H 4.51, N 12.73.

2-(2,4-dichlorophenyl)-4-phenyl-1,2-dihydroquinazoline [44] **(6f)** : Yellow solid; FT-IR (KBr) ν cm^{-1} : 3395, 3064, 2921, 2225, 1616, 1472, 1336, 1249, 1099, 912, 697 and 533; ^{1}H NMR ($CDCl_3$, 400 MHz): δ 8.18 (t, *J*=8.0 Hz, 1H), 7.91-7.89 (m, 1H), 7.73 (d, *J*=8.0 Hz, 1H), 7.61-7.57 (m, 2H), 7.44-7.43 (m, 2H), 7.41 (s, 1H), 7.26-7.24 (m, 1H), 7.20-7-18 (m, 1H), 6.73 (t, *J*=8.0 Hz, 1H), 6.66 (d, *J*=8.0 Hz, 1H), 6.31 (s, 1H), 4.22 (s, 1H); ^{13}C NMR ($CDCl_3$, 100 MHz): δ 167.03, 151.76, 146.73, 137.99, 135.64, 134.68, 134.07, 131.01, 130.30, 129.48, 121.47, 118.73, 117.81, 114.57, 68.53; CHN analysis (Mol. Formula $C_{20}H_{14}Cl_2N_2$): calculated (%) C 68.00, H 3.99, N 7.93; Found (%) C 67.96, H 3.97, N 7.89.

2,4-diphenyl-1,2-dihydroquinazoline [43] **(6g)** : Yellow solid; FT-IR (KBr) ν cm^{-1} : 3442, 3065, 2923, 1612, 1541, 1484, 1341, 1249, 1028, 764, 700, 537; ^{1}H NMR ($CDCl_3$, 400 MHz): δ 7.62-7.56 (m, 5H), 7.44-7.38 (m, 3H), 7.36-7.33 (m, 1H), 7.24 (d, *J*=8.0 Hz, 2H), 7.17 (d, *J*=8.0 Hz, 1H), 6.71 (t, *J*=8.0 Hz, 1H), 6.67 (d, *J*=8.0 Hz, 1H), 5.94 (s, 1H), 4.38 (s, 1H); ^{13}C NMR ($CDCl_3$, 100 MHz): δ 165.87, 146.89, 142.59, 138.17, 130.28, 129.30, 128.72, 128.18, 127.40, 118.31, 117.95, 114.33, 100.02, 72.70; CHN analysis (Mol. Formula $C_{20}H_{16}N_2$): calculated (%) C 84.48, H 5.67, N 9.85; Found (%) C 84.41, H 5.62, N 9.83.

2-(4-methoxyphenyl)-4-phenyl-1,2-dihydroquinazoline [45, 70] **(6h)** : Yellow solid; FT-IR (KBr) ν cm^{-1} : 3449, 3065, 2936, 2346, 1612, 1513, 1448, 1314, 1028, 751, 700, 537; ^{1}H NMR ($CDCl_3$, 400 MHz): δ 8.65 (d, *J*=8.0 Hz, 1H), 7.59-7.54 (m, 2H), 7.51-7.49 (m, 2H), 7.43-7.39 (m, 1H), 7.24-7.22 (m, 1H), 7.15 (d, *J*=8.0 Hz, 1H), 7.04-7.01 (m, 1H), 6.91 (d, *J*=8.0 Hz, 2H), 6.70 (t, *J*=8.0 Hz, 1H), 6.66 (d, *J*=8.0 Hz, 1H), 5.89 (s, 1H), 4.25 (s, 1H), 3.79 (s, 3H); ^{13}C NMR ($CDCl_3$, 100 MHz): δ 168.33, 161.85, 160.17, 158.92, 152.17, 151.67, 140.56, 137.86, 135.62, 130.61, 130.26, 129.15, 128.59, 128.13, 121.51, 117.53, 114.23, 112.08, 55.45; CHN analysis (Mol. Formula $C_{21}H_{18}N_2O$): calculated (%) C 80.23, H 5.77, N 8.91; Found (%) C 80.21, H 5.71, N 8.85.

2.4.6. Spectra of N,N'-Disulfopiperazinium chloride

a) FT-IR spectrum of [DSPZ].2Cl

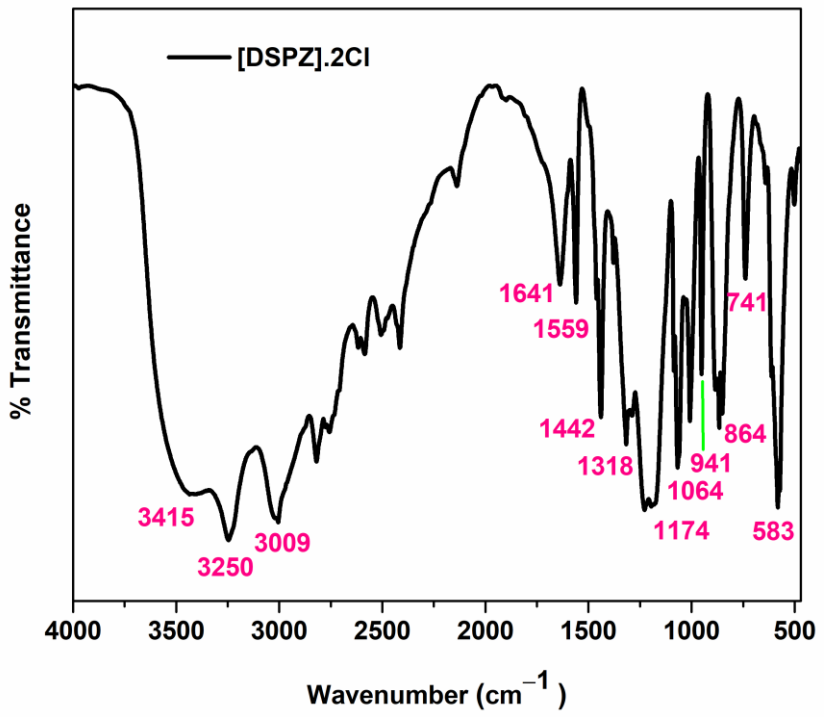

b) ^{1}H NMR spectrum of [DSPZ].2Cl

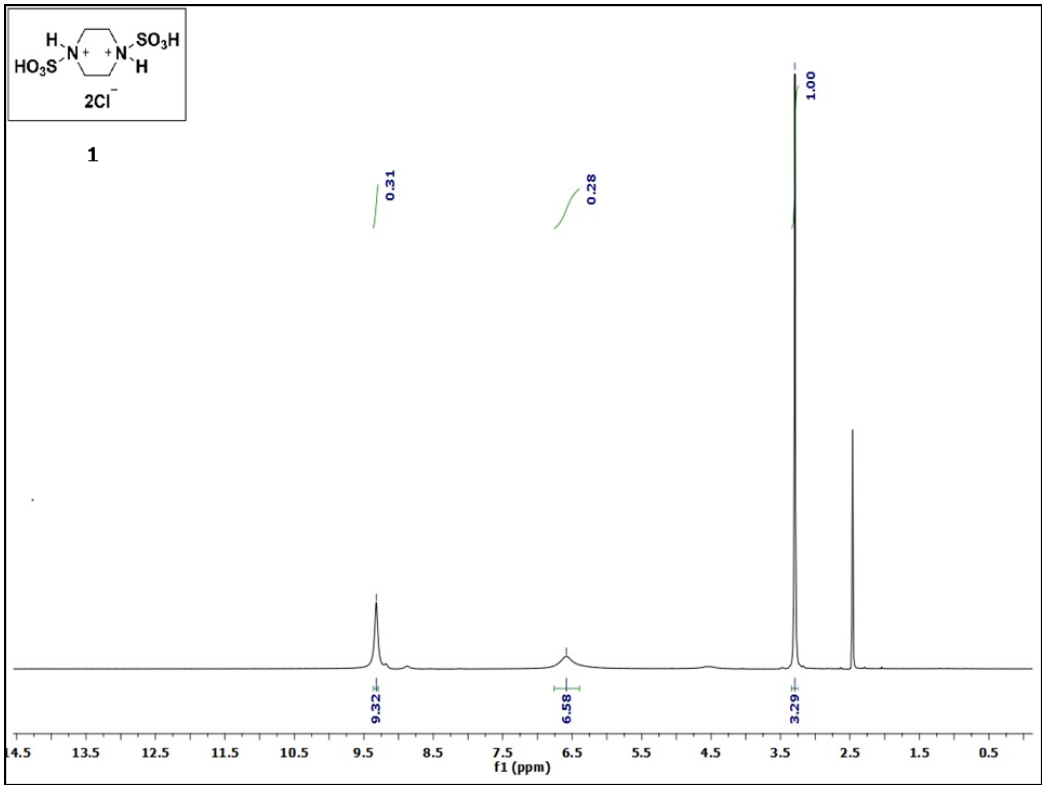

c) ^{13}C NMR spectrum of [DSPZ].2Cl

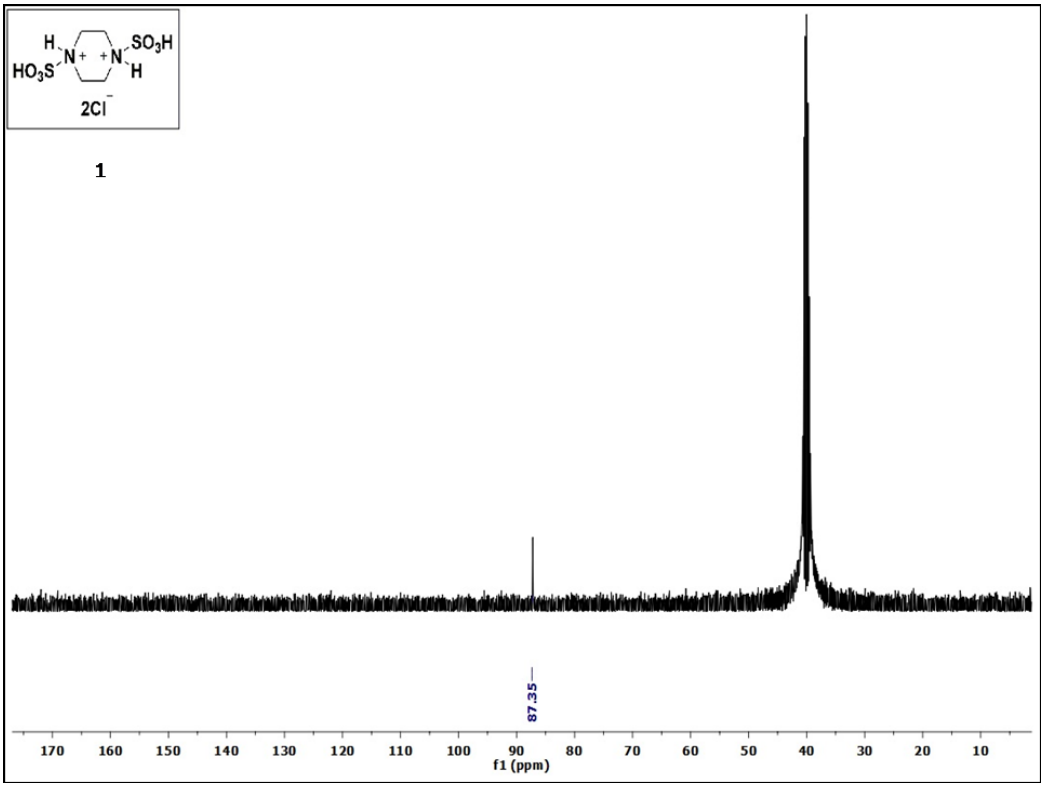

2.4.7. ^{1}H NMR spectra of 1,2-dihydroquinazoline products (6a-h)

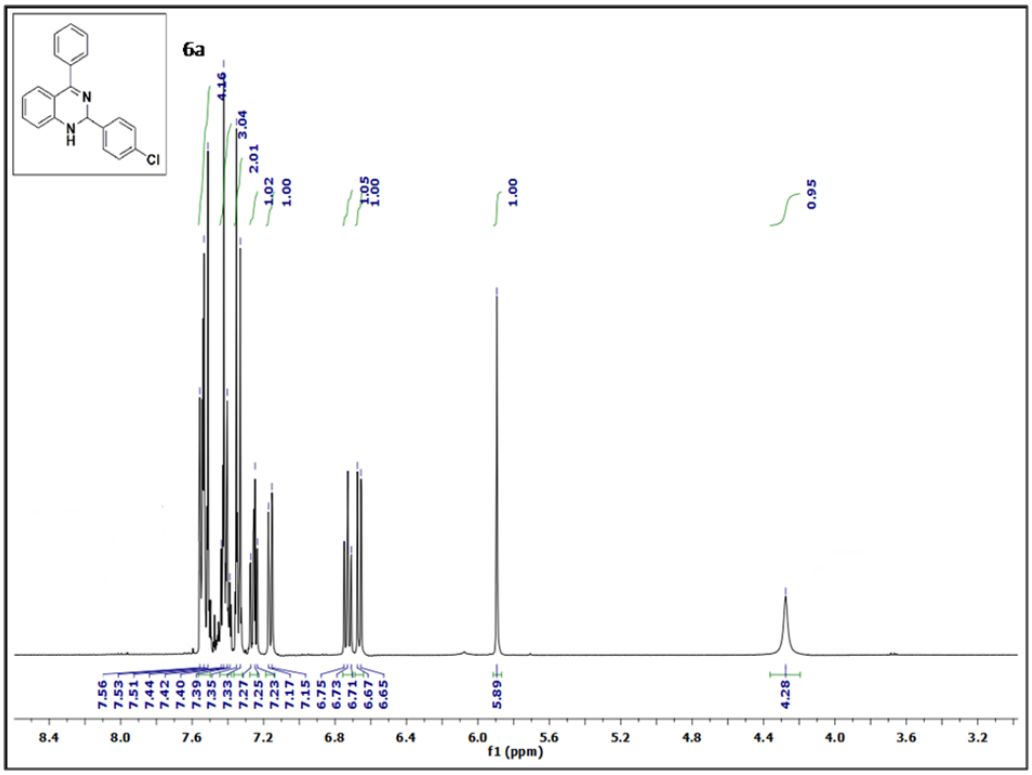

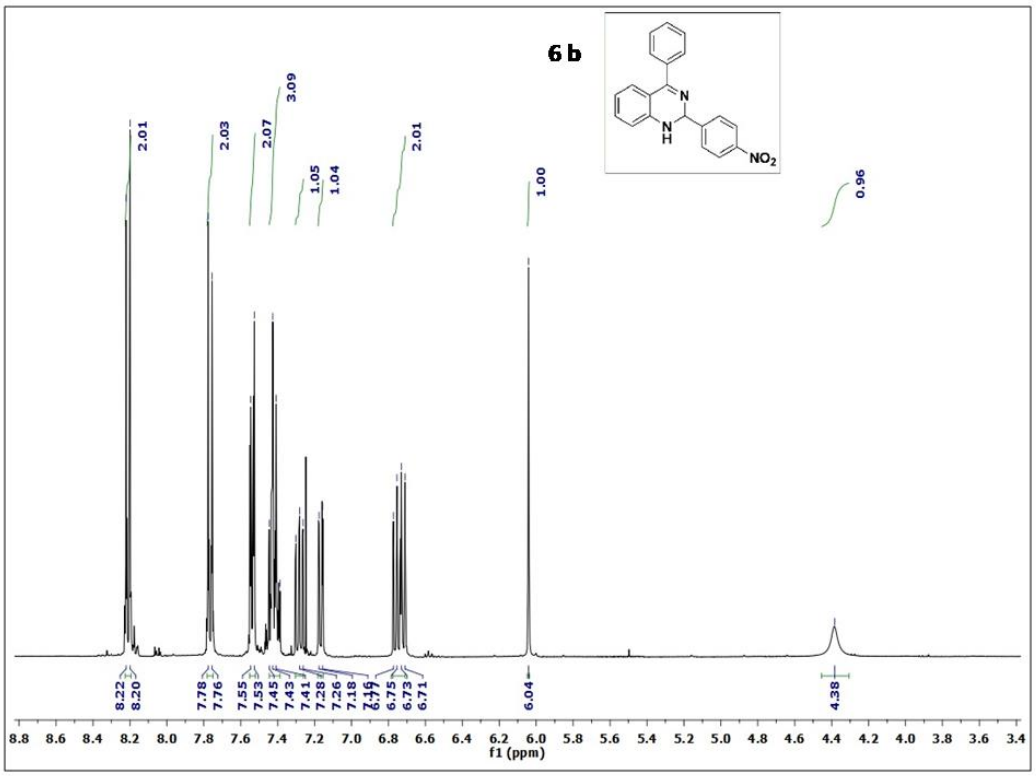
6 b
N
N
H
NO2
2.01
2.03
2.07
3.09
1.05
1.04
2.01
1.00
0.96
8.22
8.20
7.78
7.76
7.55
7.53
7.45
7.43
7.41
7.28
7.26
7.18
7.16
6.75
6.73
6.71
6.04
4.38
f1 (ppm)

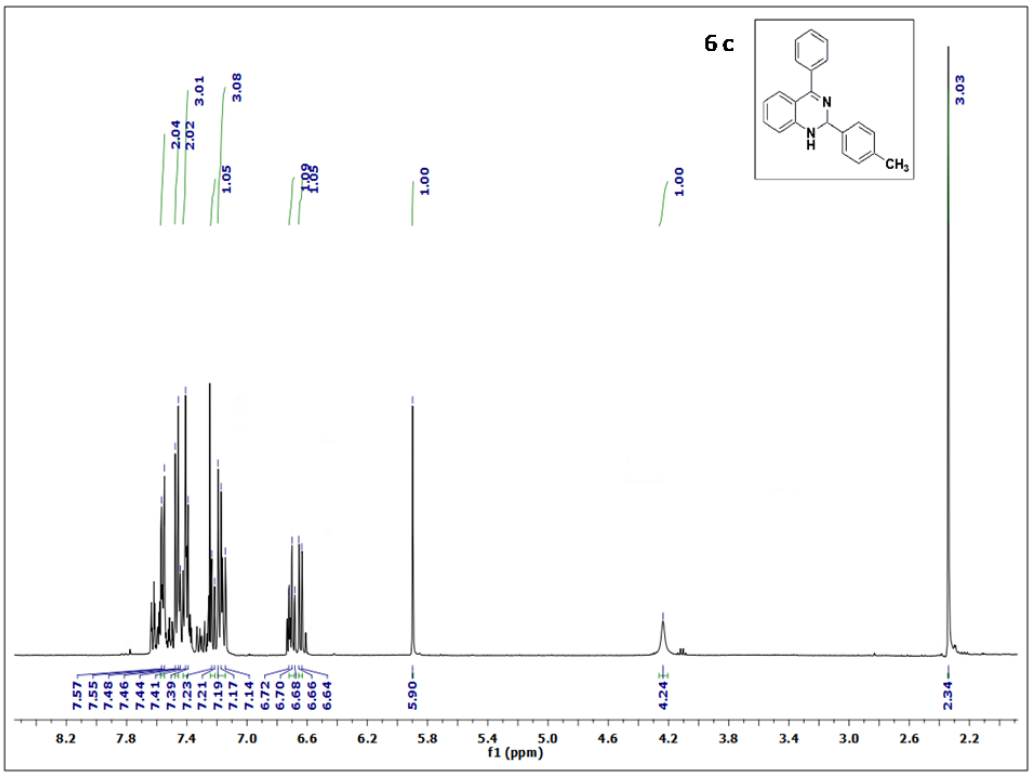
6 c
N
N
H
CH3
2.04
2.02
3.01
3.08
1.05
1.00
1.00
3.03
7.57
7.55
7.48
7.46
7.44
7.41
7.39
7.23
7.21
7.19
7.17
7.14
6.72
6.70
6.68
6.66
6.64
5.90
4.24
2.34
f1 (ppm)

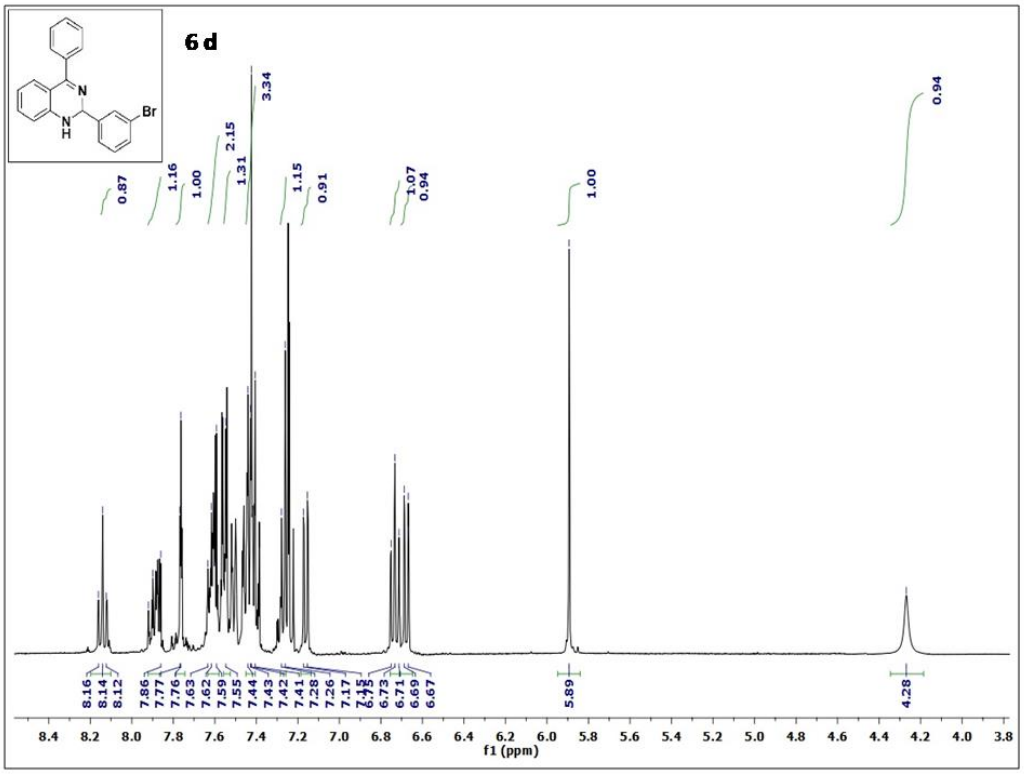
6d
Br
N
H
f1 (ppm)

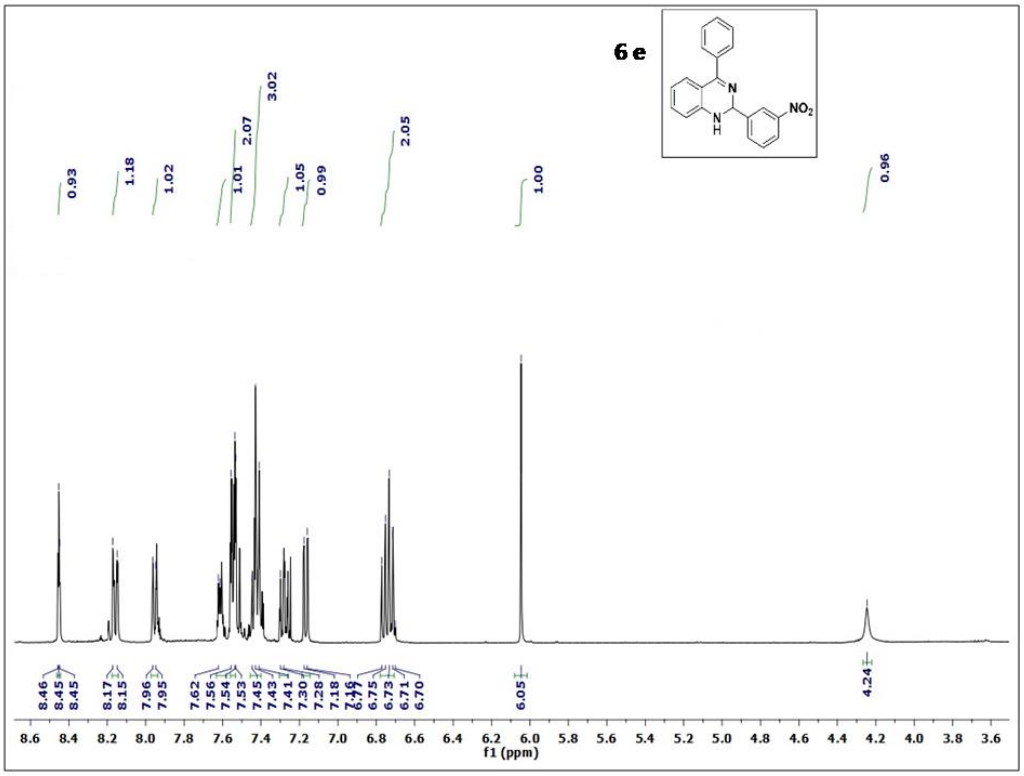
6e
NO2
N
H
f1 (ppm)

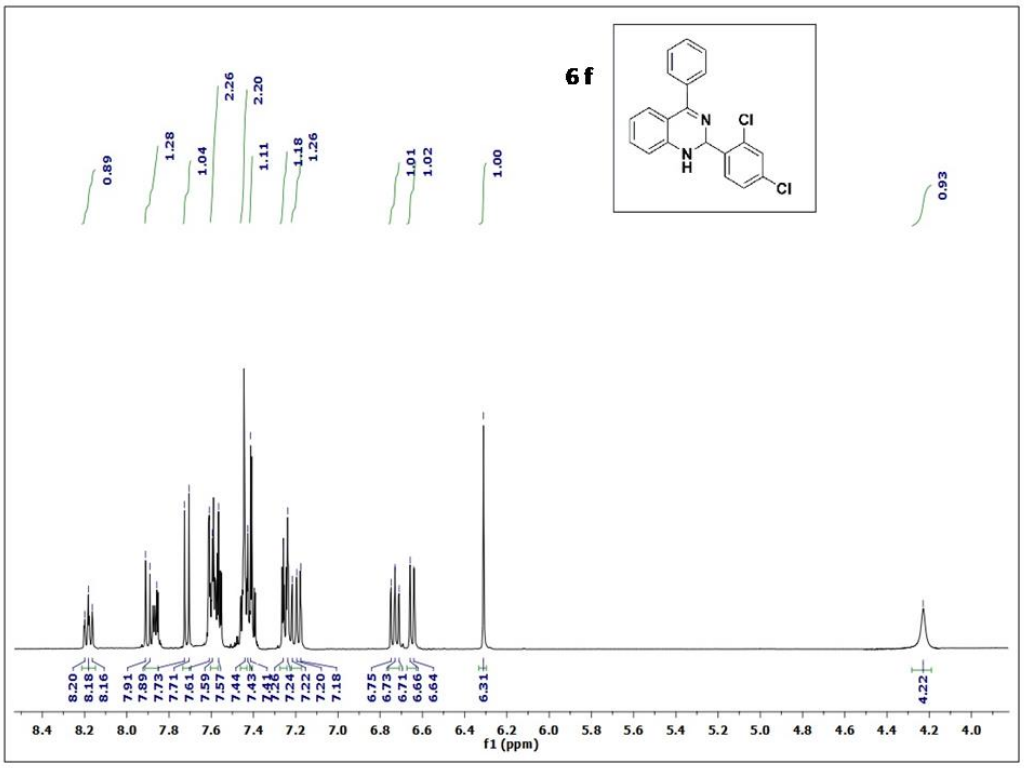
6f
Cl
Cl
N
H
f1 (ppm)

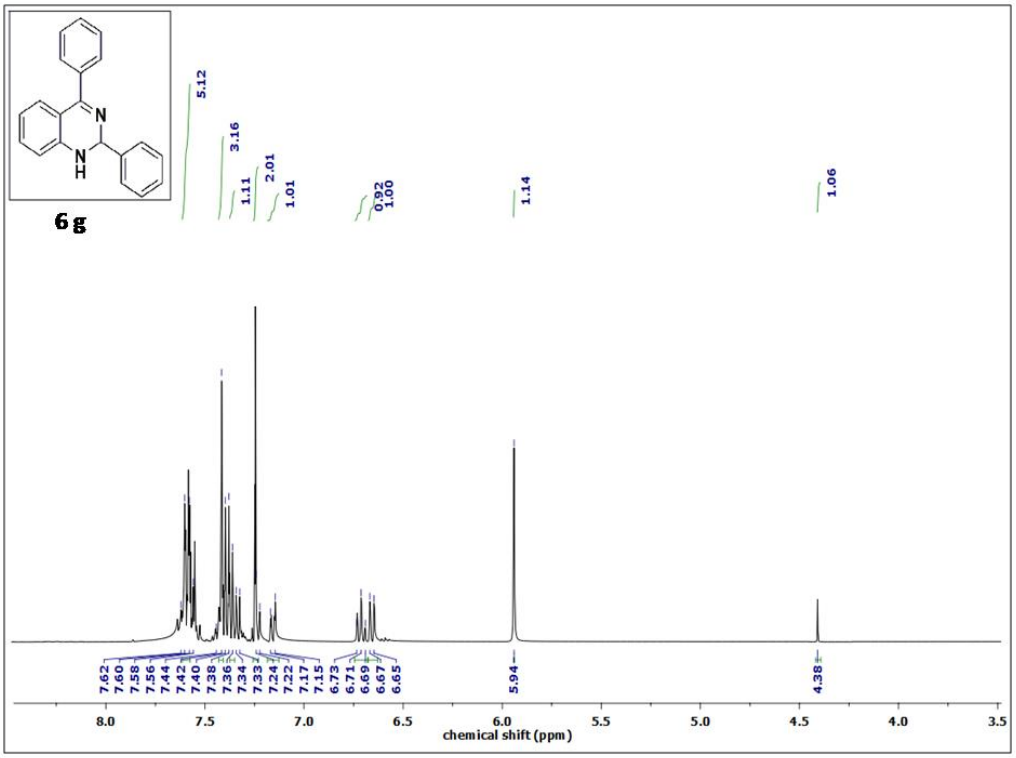
6g
N
H
chemical shift (ppm)

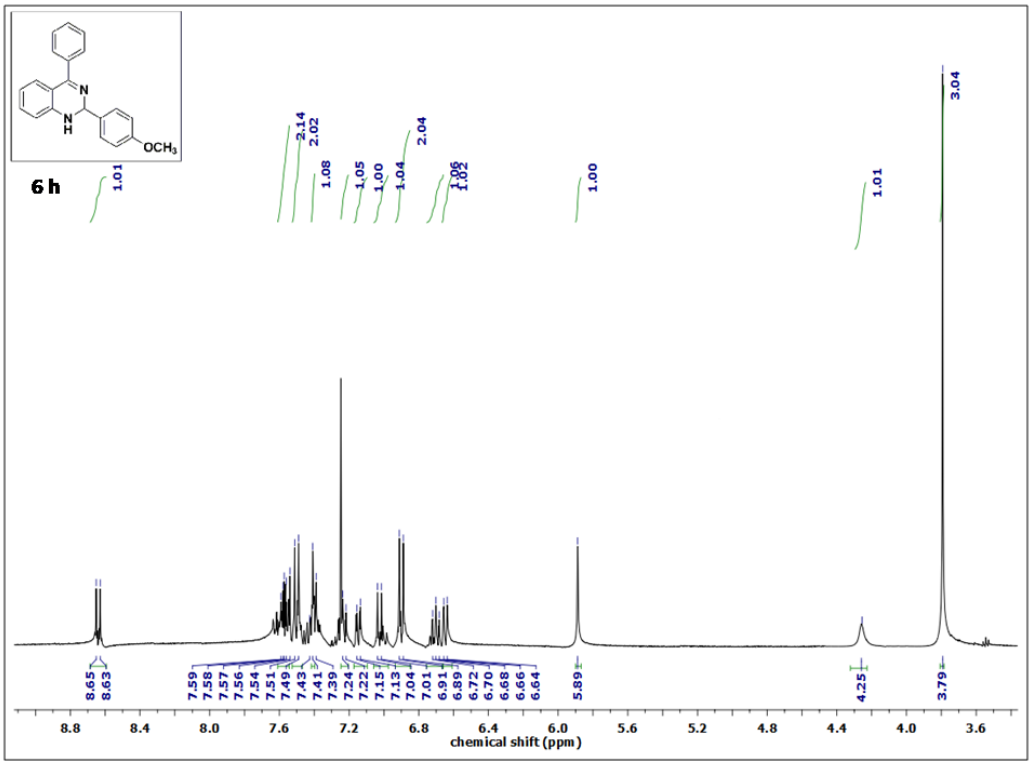

2.4.8. ^{13}C NMR spectra of 1,2-dihydroquinazoline products (6a-h)

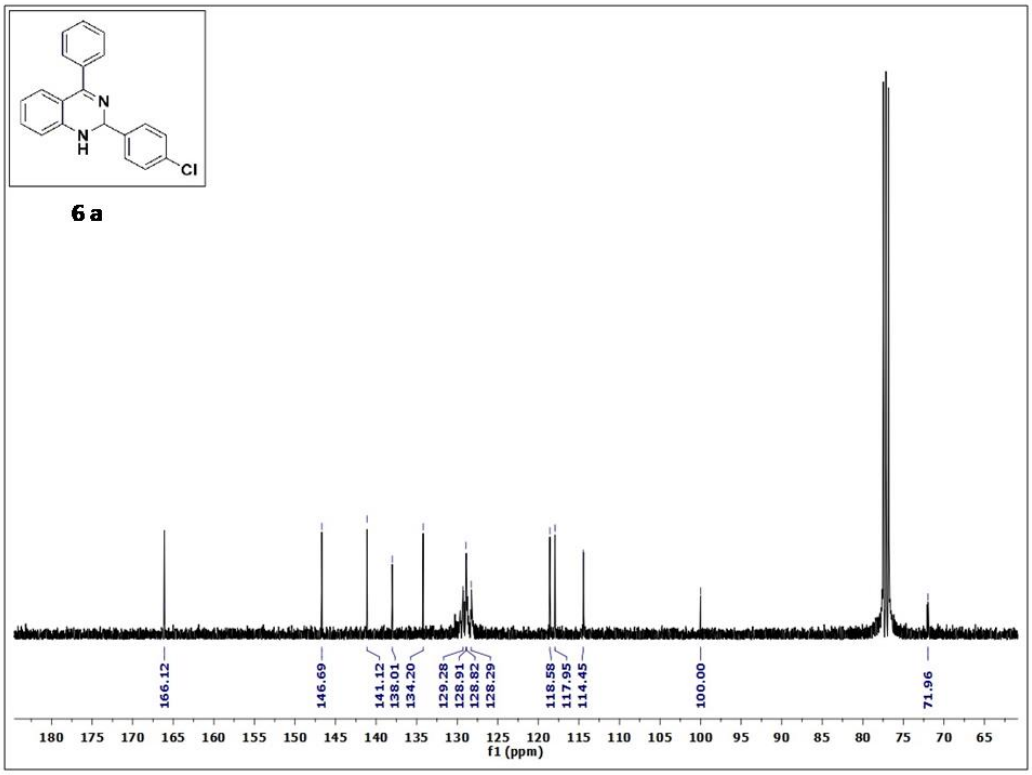

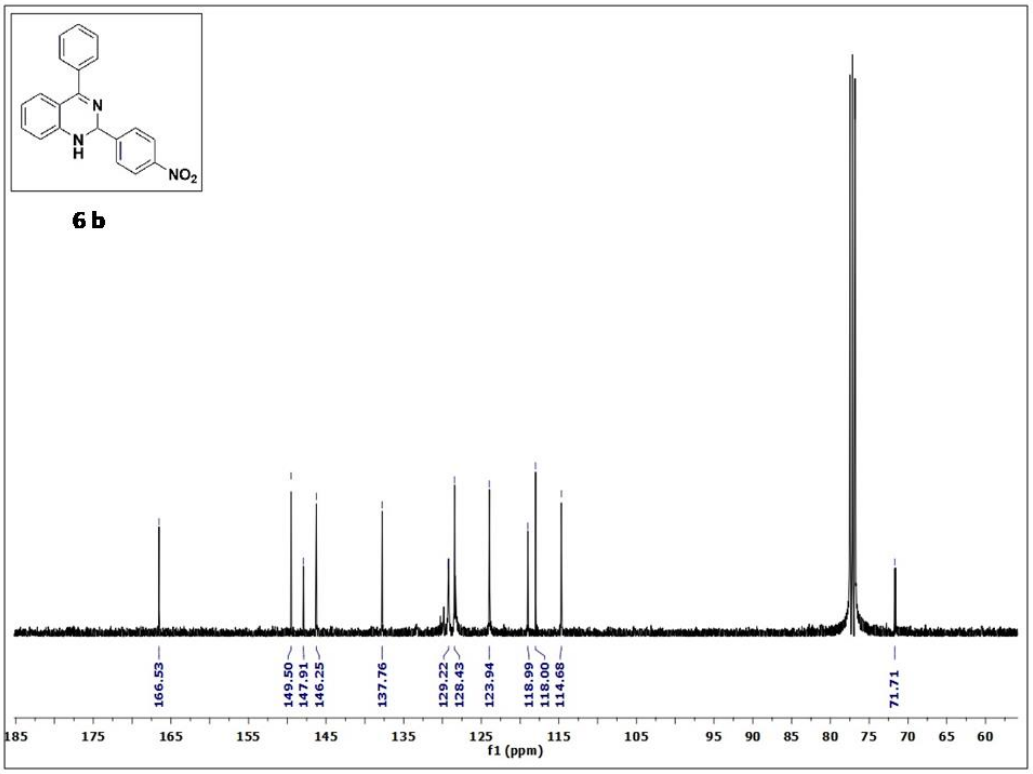
6 b
166.53
149.50
147.91
146.25
137.76
129.22
128.43
123.94
118.99
118.00
114.68
71.71
f1 (ppm)

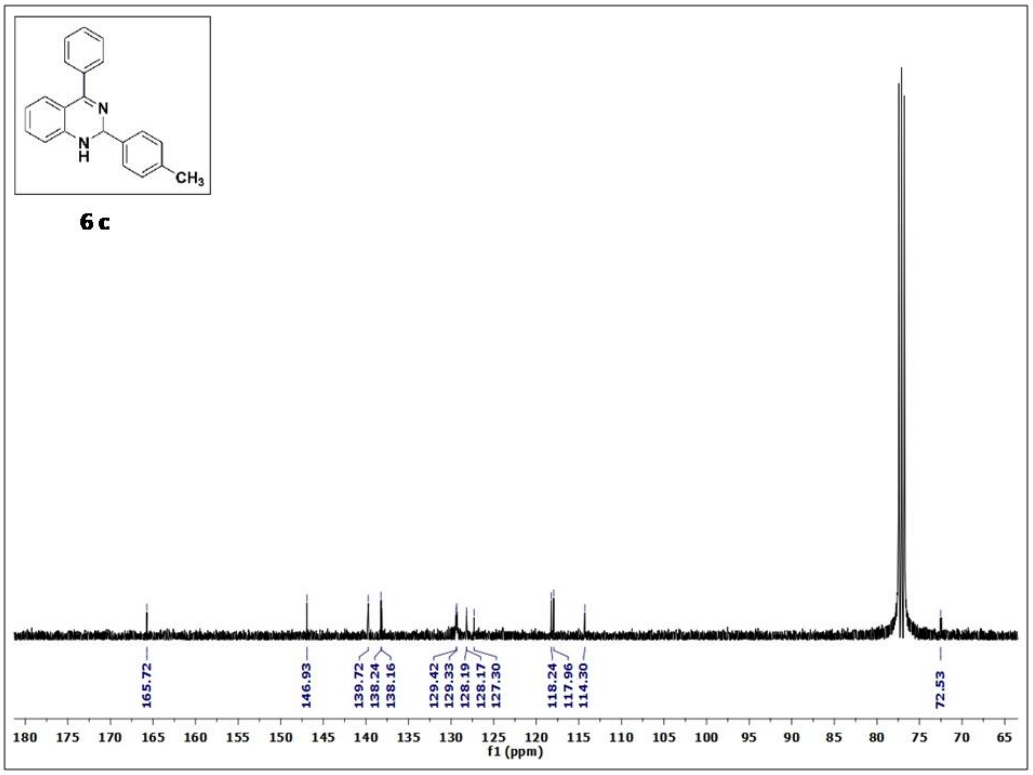
6 c
165.72
146.93
139.72
138.24
138.16
129.42
129.33
128.19
128.17
127.30
118.24
117.96
114.30
72.53
f1 (ppm)

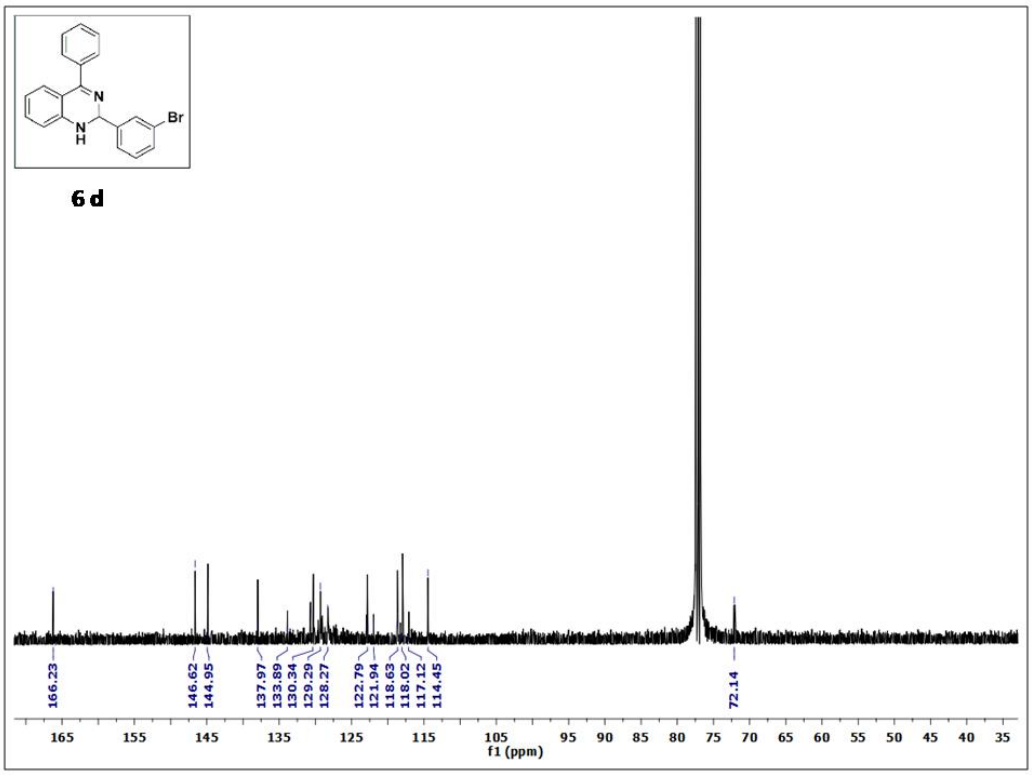
Br
6d
166.23
146.62
144.95
137.97
133.89
130.34
129.29
128.27
122.79
121.94
118.63
118.02
117.12
114.45
72.14
f1 (ppm)

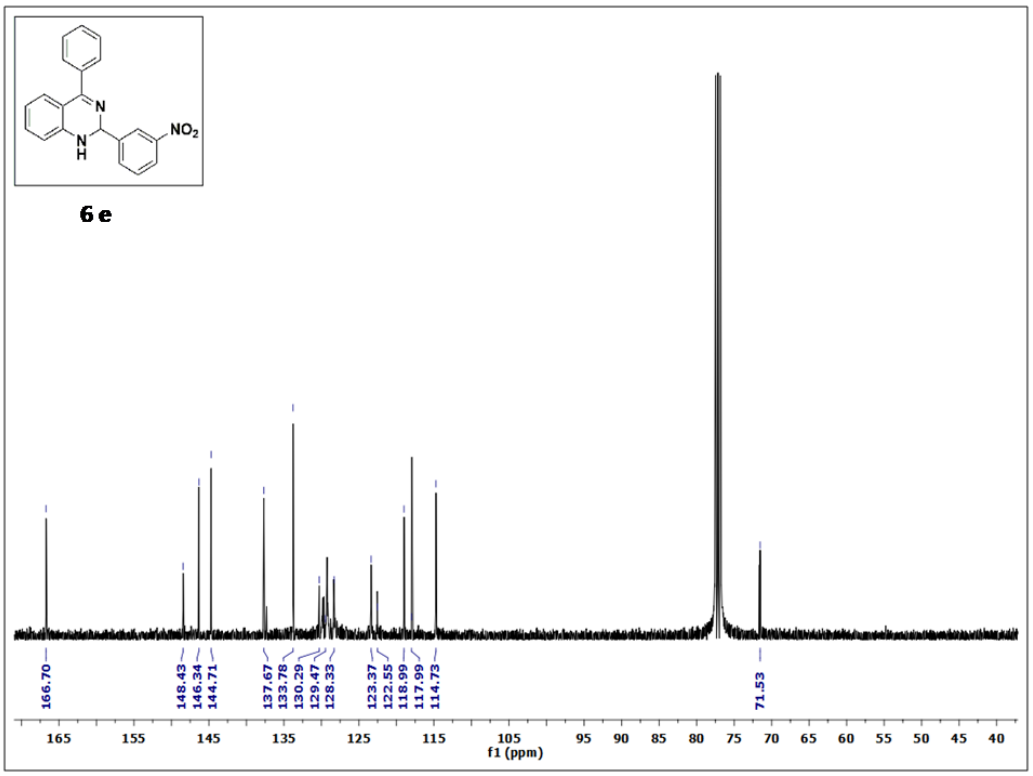
NO2
6e
166.70
148.43
146.34
144.71
137.67
133.78
130.29
129.47
128.33
123.37
122.55
118.99
117.99
114.73
71.53
f1 (ppm)

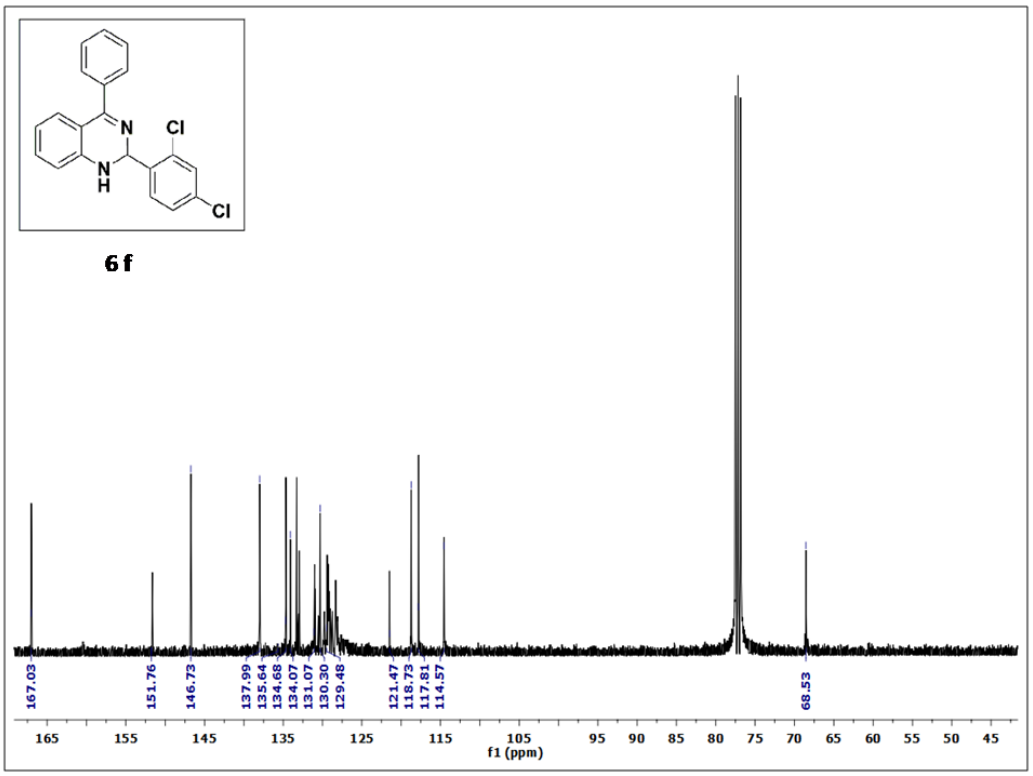
N
Cl
N
H
Cl
6 f
167.03
151.76
146.73
137.99
135.64
134.68
134.07
131.07
130.30
129.48
121.47
118.73
117.81
114.57
68.53
165
155
145
135
125
115
105
95
90
85
80
75
70
65
60
55
50
45
f1 (ppm)

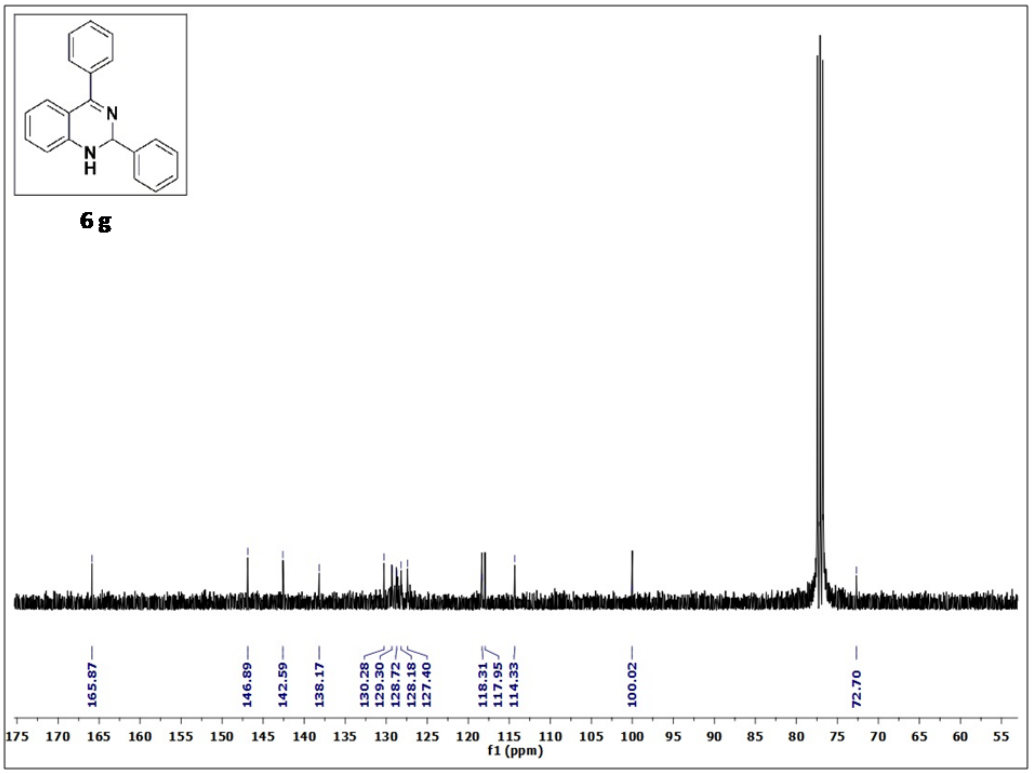
N
N
H
6 g
165.87
146.89
142.59
138.17
130.28
129.30
128.72
128.18
127.40
118.31
117.95
114.33
100.02
72.70
175
170
165
160
155
150
145
140
135
130
125
120
115
110
105
100
95
90
85
80
75
70
65
60
55
f1 (ppm)

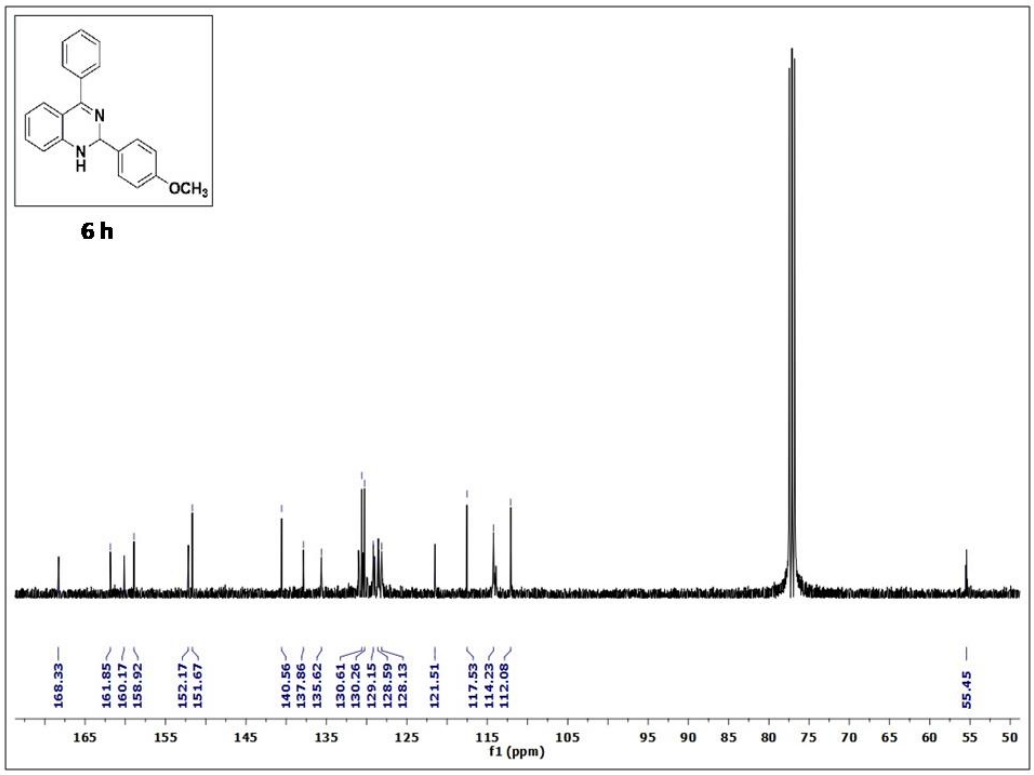

2.5. Bibliography

[1] Estager, J., Holbrey, J. D., and Swadźba-Kwaśny, M. Halometallate ionic liquids–revisited. *Chemical Society Reviews*, 43(3):847-886, 2014.

[2] Jankowska-Wajda, M., Bartlewicz, O., Pietras, P., and Maciejewski, H. Piperidinium and pyrrolidinium ionic liquids as precursors in the synthesis of new platinum catalysts for hydrosilylation. *Catalysts*, 10(8):19, 2020.

[3] Currie, M., Estager, J., Licence, P., Men, S., Nockemann, P., Seddon, K. R., Swadźba-Kwaśny, M., and Terrade, C. Chlorostannate (II) ionic liquids: Speciation, Lewis acidity, and oxidative stability. *Inorganic Chemistry*, 52(4):1710-1721, 2013.

[4] Estager, J., Oliferenko, A. A., Seddon, K. R., and Swadźba-Kwaśny, M. Chlorometallate (iii) ionic liquids as Lewis acidic catalysts-a quantitative study of acceptor properties. *Dalton Transactions*, 39(47):11375-11382, 2010.

[5] Kore, R., Berton, P., Kelley, S. P., Aduri, P., Katti, S. S., and Rogers, R. D. Group IIIA halometallate ionic liquids: Speciation and applications in catalysis. *ACS Catalysis*, 7(10):7014-7028, 2017.

[6] Brown, L. C., Hogg, J. M., and Swadźba-Kwaśny, M. Lewis acidic ionic liquids. *Topic in Current Chemistry (Z)*, 375:78, 2017.

[7] Hayashi, S. and Hamaguchi, H. O. Discovery of a magnetic ionic liquid [bmim] $FeCl_4$. *Chemistry Letters*, 33(12):1590-1591, 2004.

[8] Clarke, C. J., Baaqel, H., Matthews, R. P., Chen, Y., Lovelock, K. R., Hallett, J. P., and Licence, P. Halometallate ionic liquids: Thermal properties, decomposition pathways, and life cycle considerations. *Green Chemistry*, 24(15):5800-5812, 2022.

[9] Saikia, S., Gogoi, P., Dutta, A. K., Sarma, P., and Borah, R. Design of multifaceted acidic 1, 3-disulfoimidazolium chlorometallate ionic systems as heterogeneous catalysts for the preparation of β-amino carbonyl compounds. *Journal of Molecular Catalysis A: Chemical*, 416:63-72, 2016.

[10] Lin, M. C., Gong, M., Lu, B., Wu, Y., Wang, D. Y., Guan, M., Angell, M., Chen, C., Yang, J., Hwang, B. J., and Dai, H. An ultrafast rechargeable aluminium-ion battery. *Nature*, 520(7547):324-328, 2015.

[11] Li, X., Zhao, D., Fei, Z., and Wang, L. Applications of functionalized ionic liquids. *Science in China Series B: Chemistry*, 49:385-401, 2006.

[12] Gogoi, P., Dutta, A.K., Sarma, P., and Borah, R. Development of Brönsted–Lewis acidic solid catalytic system of 3-methyl-1-sulfonic acid imidazolium transition metal chlorides for the preparation of bis (indolyl) methanes. *Applied Catalysis A: General*, 492:133-139, 2015.

[13] Dutta, A. K., Gogoi, P., and Borah, R. Diethyldisulfoammonium chlorometallates as heterogeneous Brønsted–Lewis acidic catalysts for one-pot synthesis of 14-aryl-7-(N-phenyl)-14H-dibenzo [a, j] acridines. *Applied Organometallic Chemistry*, 32(1):e3900, 2018.

[14] Dutta, A. K., Boruah, K., and Borah, R. Development of N,N-disulfo-1,1,3,3-tetramethylguanidinium chlorometallates as heterogeneous catalysts for one pot synthesis of 1,2-dihydro-1-aryl-3H-naphth[1,2-e][1,3]oxazin-3-one derivatives. *Current Organocatalysis*, 8(2):172-186, 2021.

[15] Anderson, J. L., Ding, R., Ellern, A., and Armstrong, D. W. Structure and properties of high stability geminal dicationic ionic liquids. *Journal of the American Chemical Society*, 127(2):593-604, 2005.

[16] Shirota, H., Mandai, T., Fukazawa, H., and Kato, T. Comparison between dicationic and monocationic ionic liquids: Liquid density, thermal properties, surface tension, and shear viscosity. *Journal of Chemical & Engineering Data*, 56(5):2453-2459, 2011.

[17] Saikia, S. and Borah, R. One-pot sequential synthesis of 2-amino-4, 6-diaryl pyrimidines involving SO_3H-functionalized piperazinium-based dicationic ionic liquids as homogeneous catalysts. *ChemistrySelect*, 4(30):8751-8756, 2019.

[18] Koodehi, T. G., Shirini, F., and Goli-Jolodar, O. Preparation, characterization and application of 1, 4-disulfopiperazine-1, 4-diium chloride ([Piper-$(SO_3H)_2$]·2Cl) as an efficient dicationic ionic catalyst for the N-Boc protection of amines. *Journal of the Iranian Chemical Society*, 14:443-456, 2017.

[19] Asif, M. Chemical characteristics, synthetic methods, and biological potential of quinazoline and quinazolinone derivatives. *International Journal of Medicinal Chemistry*, 2014(1):395637, 2014.

[20] Hoonur, R. S., Patil, B. R., Badiger, D. S., Vadavi, R. S., Gudasi, K. B., Dandawate, P. R., Ghaisas, M. M., Padhye, S. B., and Nethaji, M. Transition metal complexes of 3-aryl-2-substituted 1, 2-dihydroquinazolin-4 (3H)-one derivatives: New class of analgesic and anti-inflammatory agents. *European Journal of Medicinal Chemistry*, 45(6):2277-2282, 2010.

[21] Saini, M. S., Kumar, A., Dwivedi, J., and Singh, R. A review: Biological significances of heterocyclic compounds. *International Journal of Pharmaceutical Sciences and Research*, 4(3):66-77, 2013.

[22] Gupta, T., Rohilla, A., Pathak, A., Akhtar, M. J., Haider, M. R., and Yar, M. S. Current perspectives on quinazolines with potent biological activities: A review. *Synthetic Communications*, 48(10):1099-1127, 2018.

[23] Huang, C., Fu, Y., Fu, H., Jiang, Y., and Zhao, Y. Highly efficient copper-catalyzed cascade synthesis of quinazoline and quinazolinone derivatives. *Chemical communications*, 47:6333-6335, 2008.

[24] Truong, V. L. and Morrow, M. Mild and efficient ligand-free copper-catalyzed condensation for the synthesis of quinazolines. *Tetrahedron Letters*, 51(4):758-760, 2010.

[25] Ohta, Y., Tokimizu, Y., Oishi, S., Fujii, N., and Ohno, H. Direct synthesis of quinazolines through copper-catalyzed reaction of aniline-derived benzamidines. *Organic Letters*, 12(17):3963-3965, 2010.

[26] Alonso, R., Caballero, A., Campos, P. J., Sampedro, D., and Rodriguez, M. A. An efficient synthesis of quinazolines: A theoretical and experimental study on the photochemistry of oxime derivatives. *Tetrahedron*, 66(25):4469-4473, 2010.

[27] Zhang, J., Zhu, D., Yu, C., Wan, C., and Wang, Z. A simple and efficient approach to the synthesis of 2-phenylquinazolines via sp^3 C−H functionalization. *Organic Letters*, 12(12):2841-2843, 2010.

[28] Han, B., Wang, C., Han, R. F., Yu, W., Duan, X. Y., Fang, R., and Yang, X. L. Efficient aerobic oxidative synthesis of 2-aryl quinazolines via benzyl C–H bond amination catalyzed by 4-hydroxy-TEMPO. *Chemical Communications*, 47(27):7818-7820, 2011.

[29] Maheswari, C. U., Kumar, G. S., Venkateshwar, M., Kumar, R. A., Kantam, M. L., and Reddy, K. R. Highly efficient one-pot synthesis of 2-substituted quinazolines and 4H-benzo [d][1, 3] oxazines via cross dehydrogenative coupling using sodium hypochlorite. *Advanced Synthesis & Catalysis*, 352(2-3):341-346, 2010.

[30] Peng, Y. Y., Zeng, Y., Qiu, G., Cai, L., and Pike, V. W. A convenient one-pot procedure for the synthesis of 2-aryl quinazolines using active MnO_2 as oxidant. *Journal of Heterocyclic Chemistry*, 47(5):1240-1245, 2010.

[31] Kumar, V., Mohan, C., Gupta, M., and Mahajan, M. P. A catalyst-and solvent-free selective approach to biologically important quinazolines and benzo [g] quinazoline. *Tetrahedron,* 61(14):3533-3538, 2005.

[32] Portela-Cubillo, F., Scott, J. S., and Walton, J. C. Microwave-promoted syntheses of quinazolines and dihydroquinazolines from 2-aminoarylalkanone O-phenyl oximes. *The Journal of Organic Chemistry*, 74(14):4934-4942, 2009.

[33] Moghimi, A., Khanmiri, R. H., Omrani, I., and Shaabani, A. A new library of 4 (3H)-and 4, 4′(3H, 3H′)-quinazolinones and 2-(5-alkyl-1, 2, 4-oxadiazol-3-yl) quinazolin-4 (3H)-one obtained from diaminoglyoxime. *Tetrahedron Letters*, 54(30):3956-3959, 2013.

[34] Guo, S., Zhai, J., Wang, F., and Fan, X. One-pot three-component selective synthesis of isoindolo [2, 1-a] quinazoline derivatives via a palladium-catalyzed cascade cyclocondensation/cyclocarbonylation sequence. *Organic & Biomolecular Chemistry*, 15(17):3674-3680, 2017.

[35] Wang, C., Li, S., Liu, H., Jiang, Y. and Fu, H. Copper-catalyzed synthesis of quinazoline derivatives via ullmann-type coupling and aerobic oxidation. *The Journal of Organic Chemistry*, 75(22):7936-7938, 2010.

[36] Ghorbani-Vaghei, R., Shirzadi-Ahodashti, M., Eslami, F., Malaekehpoor, S. M., Salimi, Z., Toghraei-Semiromi, Z., and Noori, S. Efficient one-pot synthesis of quinazoline and benzopyrano [2, 3-d] pyrimidine derivatives catalyzed by n-bromosulfonamides. *Journal of Heterocyclic Chemistry*, 54(1):215-225, 2017.

[37] Maleki, A., Rabbani, M., and Shahrokh, S. Preparation and characterization of a silica-based magnetic nanocomposite and its application as a recoverable catalyst for the one-pot multicomponent synthesis of quinazolinone derivatives. *Applied Organometallic Chemistry*, 29(12):809-814, 2015.

[38] Dabiri, M., Salehi, P., and Bahramnejad, M. Ecofriendly and efficient one-pot procedure for the synthesis of quinazoline derivatives catalyzed by an acidic ionic liquid under aerobic oxidation conditions. *Synthetic Communications*, 40(21):3214-3225, 2010.

[39] Panja, S. K. and Saha, S. Recyclable, magnetic ionic liquid bmim $[FeCl_4]^-$ catalyzed, multicomponent, solvent-free, green synthesis of quinazolines. *RSC Advances*, 3(34):14495-14500, 2013.

[40] Fatehi, A., Ghorbani-Vaghei, R., Alavinia, S., and Mahmoodi, J. Synthesis of quinazoline derivatives catalyzed by a new efficient reusable nanomagnetic catalyst supported with functionalized piperidinium benzene-1, 3-disulfonate ionic liquid. *ChemistrySelect*, 5(3):944-951, 2020.

[41] Portela-Cubillo, F., Scott, J. S., and Walton, J. C. 2-(Aminoaryl) alkanone O-phenyl oximes: versatile reagents for syntheses of quinazolines. *Chemical Communications*, 25:2935-2937, 2008.

[42] Sarma, R. and Prajapati, D. Microwave-promoted efficient synthesis of dihydroquinazolines. *Green Chemistry*, 13(3):718-722, 2011.

[43] Derabli, C., Boulcina, R., Kirsch, G., Carboni, B., and Debache, A. A DMAP-catalyzed mild and efficient synthesis of 1, 2-dihydroquinazolines via a one-pot three-component protocol. *Tetrahedron Letters*, 55(1):200-204, 2014.

[44] Gudimella, K. K., Bonige, K. B., Gundla, R., Katari, N. K., Yamajala, B., and Battula, V. R. 2, 4-Diphenyl-1, 2-dihydroquinazoline Derivatives: Synthesis, Anticancer Activity and Docking Studies. *ChemistrySelect*, 4(43):12528-12533, 2019.

[45] Kamal, A., Babu, K. S., Poornachandra, Y., Nagaraju, B., Hussaini, S. A., Shaik, S. P., Kumar, C. G., and Alarifi, A. Efficient and green sulfamic acid catalyzed synthesis of new 1, 2-dihydroquinazoline derivatives with antibacterial potential. *Arabian Journal of Chemistry*, 12(8):3546-3554, 2019.

[46] Mueller, R., Kammler, H. K., Wegner, K., and Pratsinis, S. E. OH surface density of SiO_2 and TiO_2 by thermogravimetric analysis. *Langmuir*, 19(1):160-165, 2003.

[47] Kogelnig, D., Stojanovic, A., Kammer, F. v. d., Terzieff, P., Galanski, M. S., Jirsa, F., Krachler, R., Hofmann, T., and Keppler, B. K. Tetrachloroferrate containing ionic liquids: Magnetic-and aggregation behavior. *Inorganic Chemistry Communications*, 13(12):1485-1488, 2010.

[48] Bäcker, T., Breunig, O., Valldor, M., Merz, K., Vasylyeva, V., and Mudring, A. V. In-situ crystal growth and properties of the magnetic ionic liquid $[C_2mim][FeCl_4]$. *Crystal Growth & Design*, 11(6):2564-2571, 2011.

[49] Kistenmacher, T. T. and Stucky, G. D. Structural and spectroscopic studies of tetrachlorophosphonium tetrachloroferrate (III), $[PCl_4][FeCl_4]$. *Inorganic Chemistry*, 7(10):2150-2155, 1968.

[50] Amphlett, J. T. M., Ogden, M. D., Yang, W., and Choi, S. Probing Ni^{2+} and Co^{2+} speciation in carboxylic acid based deep eutectic solvents using UV/Vis and FT-IR spectroscopy. *Journal Of Molecular Liquids*, 318:114217, 2020.

[51] Hitchcock, P. B., Seddon, K. R., and Welton, T. Hydrogen-bond acceptor abilities of tetrachlorometalate (II) complexes in ionic liquids. *Journal of the Chemical Society, Dalton Transactions*, 17:2639-2643, 1993.

[52] Goodgame, D. M. L., Goodgame, M., and Cotton, F. A. Electronic spectra of some tetrahedral nickel (II) complexes. *Journal of the American Chemical Society*, 83(20):4161-4167, 1961.

[53] Wei, X., Yu, L., Wang, D., Jin, X., and Chen, G. Z. Thermo-solvatochromism of chloro-nickel complexes in 1-hydroxyalkyl-3-methyl-imidazolium cation based ionic liquids. *Green Chemistry*, 10(3):296-305, 2008.

[54] Khokhryakov, A. A., Mikhaleva, M. V., and Paivin, A. S. Electronic absorption spectra of nickel dichloride and nickel oxide solutions in the 2CsCl-NaCl and KCl-NaCl metls. *Russian Journal of Inorganic Chemistry*, 51:1311-1314, 2006.

[55] Angell, C. A. and Gruen, D. M. Octahedral-tetrahedral coordination equilibria of nickel (II) and copper (II) in concentrated aqueous electrolyte solutions. *Journal of the American Chemical Society*, 88(22):5192-5198, 1966.

[56] Liu, W., Migdisov, A., and Williams-Jones, A. The stability of aqueous nickel (II) chloride complexes in hydrothermal solutions: Results of UV-Visible spectroscopic experiments. *Geochimica et Cosmochimica Acta*, 94:276-290, 2012.

[57] Lopez-Salinas, E. and Ono, Y. Intercalation chemistry of a Mg-Al layered double hydroxide ion-exchanged with complex MCl_4^{2-} (M = Ni, Co) ions from organic media. *Microporous Materials*, 1(1):33-42, 1993.

[58] Kettle, S. F. A. *Physical Inorganic Chemistry: A Coordination Chemistry Approach*. Springer Berlin, Heidelberg, 1996.

[59] Rao, A. P. and Dubey, S. P. Synergistic effects in ion exchange in mixed solvents-chloride media. *Analytical Chemistry*, 44(4):686-691, 1972.

[60] Zsigrai, I. J., Gadzuric, S. B., Nikolic, R., and Nagy, L. Electronic spectra and stability of cobalt halide complexes in molten calcium nitrate tetrahydrate. *Zeitschrift für Naturforschung A*, 59(9):602-608, 2004.

[61] Binns, J., McIntyre, G. J., Barreda-Argüeso, J. A., González, J., Aguado, F., Rodríguez, F., Valiente, R., and Parsons, S. Phase transition sequences in tetramethylammonium tetrachlorometallates by X-ray diffraction and spectroscopic measurements. *Acta Crystallographica Section B: Structural Science, Crystal Engineering and Materials*, 73(5):844-855, 2017.

[62] Wang, Y. Y., Li, W., and Dai, L. Y. Brønsted acidic ionic liquids as efficient reaction medium for cyclodehydration of diethylene glycol. *Chinese Journal of Chemistry*, 26(8):1390-1394, 2008.

[63] Thomazeau, C., Olivier-Bourbigou, H., Magna, L., Luts, S., and Gilbert, B. Determination of an acidic scale in room temperature ionic liquids. *Journal of the American Chemical Society*, 125(18):5264-5265, 2003.

[64] Barzetti, T., Selli, E., Moscotti, D., and Forni, L. Pyridine and ammonia as probes for FTIR analysis of solid acid catalysts. *Journal of the Chemical Society, Faraday Transactions*, 92(8):1401-1407, 1996.

[65] Hughes, T. R. and White, H. M. A study of the surface structure of decationized Y zeolite by quantitative infrared spectroscopy. *The Journal of Physical Chemistry*, 71(7):2192-2201, 1967.

[66] Emeis, C. A. Determination of integrated molar extinction coefficients for infrared absorption bands of pyridine adsorbed on solid acid catalysts. *Journal of Catalysis*, 141(2):347-354, 1993.

[67] Selli, E. and Forni, L. Comparison between the surface acidity of solid catalysts determined by TPD and FTIR analysis of pre-adsorbed pyridine. *Microporous and mesoporous materials*, 31(1-2):129-140, 1999.

[68] Hemmann, F., Jaeger, C., and Kemnitz, E. Comparison of acidic site quantification methods for a series of nanoscopic aluminum hydroxide fluorides. *RSC Advances*, 4(100):56900-56909, 2014.

[69] Vassilyeva, O. Y., Buvaylo, E. A., Lobko, Y. V., Linnik, R. P., Kokozay, V. N., and Skelton, B. W. Organic–inorganic hybrid tetrachlorocadmates as promising fluorescent agents for cross-linked polyurethanes: Synthesis, crystal structures and extended performance analysis. *RSC Advances*, 11(13):7713-7722, 2021.

[70] Kamal, A., Babu, K. S., Chandrasekhar, C., Nagaraju, B., Sastry, K. V., and Kumar, C. G. Catalyst-free, one pot and three-component synthesis of 4′-phenyl-1′ H-spiro [indoline-3, 2′-quinazolin]-2-ones and 2, 4-diphenyl-1, 2-dihydroquinazolines. *Tetrahedron Letters*, 56(46):6373-6376, 2015.